Advancing host-directed therapy for Mycobacterium avium infection: identification of drug candidates and potential host targets

Kilinc, G.

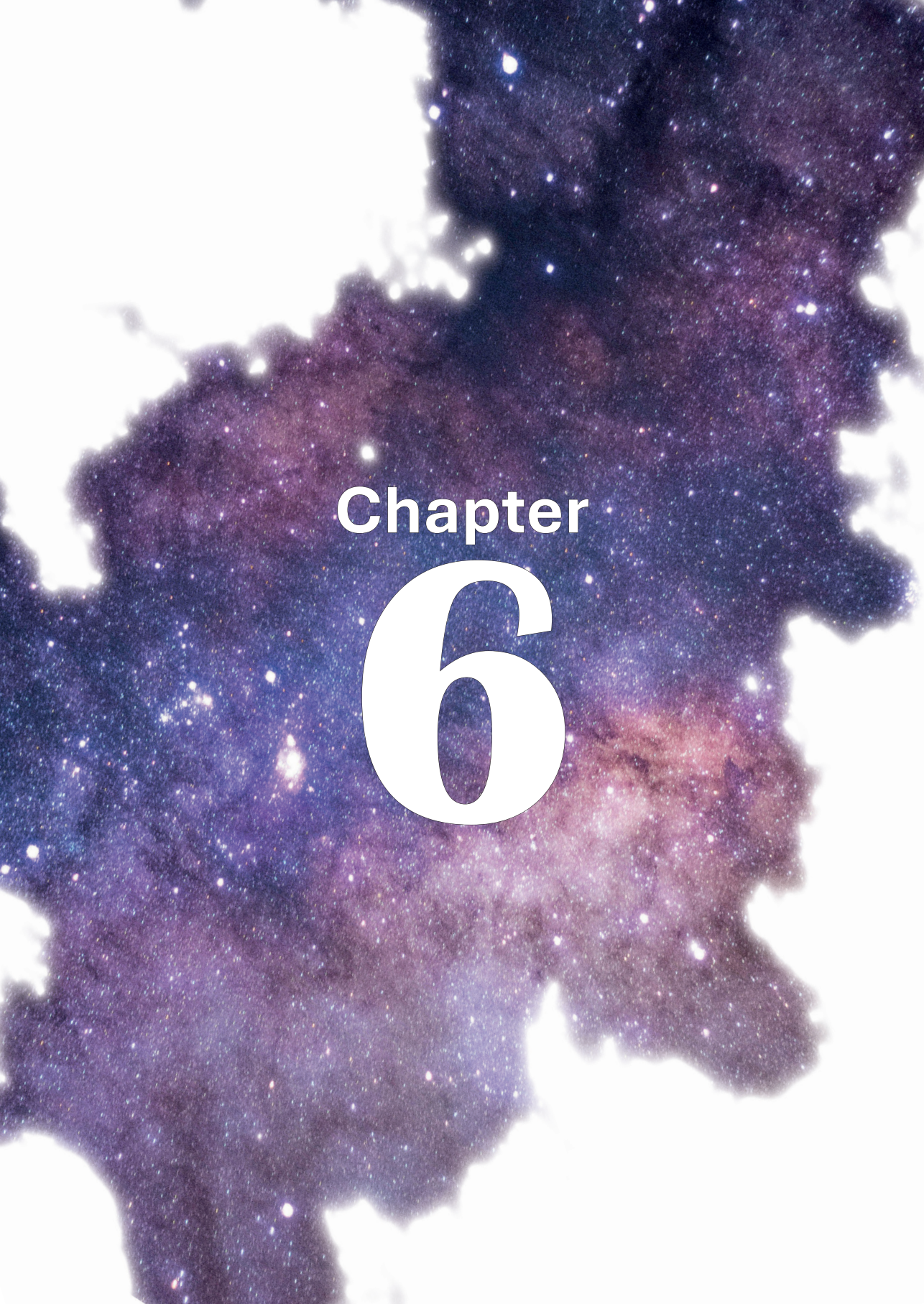

Chapter 6

Comparative transcriptomic analysis of human macrophages during *Mycobacterium avium* versus *Mycobacterium tuberculosis* infection

Gül Kilinç[1], Robin H. G. A. van den Biggelaar[1], Tom H. M. Ottenhoff[1], Leon H. Mei[2] and Anno Saris[1]

[1] Leiden University Center for Infectious Diseases, Leiden University Medical Center, Leiden, The Netherlands
[2] Department of Biomedical Data Sciences, Leiden University Medical Center, Leiden, The Netherlands

Submitted.

Abstract

The treatment of *Mycobacterium avium* (*Mav*) infection, responsible for over 80% of the chronic lung diseases caused by nontuberculous mycobacteria (NTM), remains challenging due to rising antibiotic resistance and unsatisfactory success rates. Hence, there is an urgent need for alternative treatment strategies. Host-directed therapy targets host pathways to either reduce destructive inflammation or improve antimycobacterial defenses to eradicate the infection, offering a promising approach with minimal risk of inducing drug resistance. However, compared to *Mycobacterium tuberculosis* (*Mtb*) infections, knowledge of host-pathogen interactions and development of HDT for *Mav* infection is limited. To expand our fundamental knowledge on the host response during *Mav* infections, we performed a genome-wide host transcriptomic analysis of *Mav*-infected primary human macrophages, the key players in the host immunity against *Mav*, next to *Mtb*-infected macrophages to leverage insights from *Mtb* research. Our findings show substantial overlap in the gene expression patterns between *Mav*-infected and *Mtb*-infected macrophages, including induction of cytokine responses and modulation of various G-protein coupled receptors (GPCRs) involved in (lipid-mediated) macrophage immune functions. Notably, *Mav* infection showed more pronounced modulation of nerve growth factor (NGF) signaling and genes of the GTPase of immunity-associated protein (GIMAP) family compared to *Mtb* infection. While the exact roles of these host transcriptomic responses during mycobacterial infection remain to be determined, these results may provide direction to further explore the host-pathogen interactions during *Mav*-related immunity and identify targets for HDT for the treatment of *Mav* infection.

Introduction

Mycobacterium avium (*Mav*) is the causative pathogen for the majority of the chronic lung diseases caused by nontuberculous mycobacteria (NTM) (1-3), which has seen a rise in incidence globally and is a growing public health concern (4-6). While lung disease caused by *Mav* (*Mav*-LD) particularly affects individuals with predisposing lung disorders or a compromised immune system, immunocompetent individuals with certain host characteristics have been found to develop *Mav*-LD. Improved understanding and management of NTM, in particular *Mav*, infections is therefore desirable.

The recommended treatment for *Mav*-LD consists of a three-drug antibiotic regimen comprising a macrolide, ethambutol, and a rifamycin that should be administered for at least 12 months after negative sputum conversion (7, 8). Nevertheless, even after completing the antibiotic therapy, the success rate, disappointingly, is as low as 40% (9, 10). This necessitates the development of new therapeutic strategies. One promising approach is the use of host-directed therapy (HDT), which aims to dampen destructive inflammation or to boost the host's immune responses which may be beneficial, especially for individuals who are suffering from a *Mav* infection and are immunocompromised. By targeting host immunity, HDT may help to eliminate non-replicating and drug-resistant bacteria which are hardly eradicated by antibiotic therapy. In addition, as adjunctive treatment, HDT has the potential advantage of shortening the duration or decreasing the dosage of current antibiotic regimens, which may reduce adverse drug effects. Furthermore, since host rather than bacterial pathways are targeted, the risk of de novo development of drug resistance is less likely. The development of HDT for *Mav* requires a throughout knowledge of host-pathogen interactions limited understanding of the host-pathogen interactions during *Mav* infection.

Macrophages are the immune cells that play a key role in host defense against *Mav* infection. Upon inhalation, *Mav* enters the lung alveolar space where macrophages will form the main reservoir for the mycobacteria (11, 12). Multiple macrophage receptors, including Toll-like receptors (TLRs) and C-type lectins, are involved in the initial bacterium-host cells encounter which induces phagocytosis. Upon recognition and phagocytosis, the early *Mav*-containing phagosomes undergo maturation and fusion with lysosomes containing hydrolytic enzymes to form phagolysosomes capable of eliminating the mycobacteria (13, 14). However, *Mav* is able to evade host immune surveillance and to maintain its intracellular replication and survival. For instance, the *Mav* protein *Mav*_2941 inhibits phagosome maturation, and thus prevents intracellular *Mav* killing (15, 16). The production and signaling of pro-inflammatory cytokines, including TNF, IL-12, and IL-23, by macrophages, play a vital role in further stimulating the bactericidal functions of macrophages (17). Consequently, inherited or acquired defects in the production and signaling of these cytokines lead to an increased susceptibility to *Mav*-LD (18), stressing the significant role of host immunity in deciding the outcome of *Mav* infection.

A better understanding of the mechanisms involved by which macrophages either kill *Mav* or become its breeding ground will aid the development of HDT. RNA-sequencing

has previously been used to study the macrophage host response following infection with *Mtb*, providing insights into the mechanisms of pathogenesis, potential biomarkers for disease progression, and targets for new therapeutic interventions such as HDT (19-22). In contrast, most transcriptomic studies exploring the host response to *Mav* have been conducted in cell lines, which require specific stimulation or may not accurately reflect primary human macrophage responses to mycobacteria and have relied on predefined microarray analyses that fail to reflect the complete transcriptional response (23-26). Our aim was therefore to perform genome-wide transcriptomic analysis of primary human macrophages infected with *Mav*, alongside *Mtb* as a reference to facilitate the rapid extrapolation of relevant findings from *Mtb* to *Mav*, thereby enhancing our understanding of the similarities and differences in how both pathogens interact with and are managed by the host's immune system. We hypothesized that this will ultimately contribute to the development of more effective therapies for infections caused by these mycobacteria.

In this study, we showed that the host transcriptional response is highly similar between macrophages infected with *Mav* and macrophages infected with *Mtb*. The common host response includes the expression of cytokines and other immune-related genes, but also G protein-coupled receptors involved in lipid metabolism. Furthermore, we identified genes with transcription levels that were different in magnitude between macrophages infected with *Mav* and macrophages infected with *Mtb*. These differences were linked to phospholipases, NGF signaling-related apoptosis, and the more unknown GIMAP genes.

Results

Genome-wide transcriptome analysis of primary human macrophages infected with *Mav* or *Mtb*

To investigate the induction of the early host immune response, primary human macrophages from 7 donors were infected with *Mav* or *Mtb*, with an 8th donor (*Mtb* data unavailable) maintained in the *Mav* analysis to increase power. Macrophage phagocytosis of *Mav* was higher as compared to *Mtb*, despite being exposed to a lower MOI (5.9 vs 9.9, respectively). Elimination of intracellular *Mtb* was higher at 24 hours post-infection (**Figure 1A**). Genome-wide transcriptome analysis using RNA-sequencing was performed in seven biological replicates at 2 hours and 6 hours post-infection. Expression levels were compared between infected samples and uninfected controls using unsupervised and supervised analyses. PCA analysis revealed the clustering of samples derived from different donors (**Figure 1B**), while infected samples were clustered separately from uninfected macrophages and clearly changed over time (**Figure 1C**). The transcriptome profiles of macrophages infected with either *Mav* or *Mtb* were evidently clustered together (**Figure 1D**).

Primary human macrophages infected with *Mav* or *Mtb* present similar host transcription responses

To determine the transcriptomic response upon *Mav* and *Mtb* infection, significantly differentially expressed gene (DEGs) (cutoffs: log2(fold change) ≥ 1.5 or ≤ -1.5 and false discovery rate (FDR) adjusted p-values < 0.05) were assessed by comparing gene expression levels in infected macrophages at 2 and 6 hours post-infection with uninfected controls. At 2 hours post-infection, macrophages showed downregulation

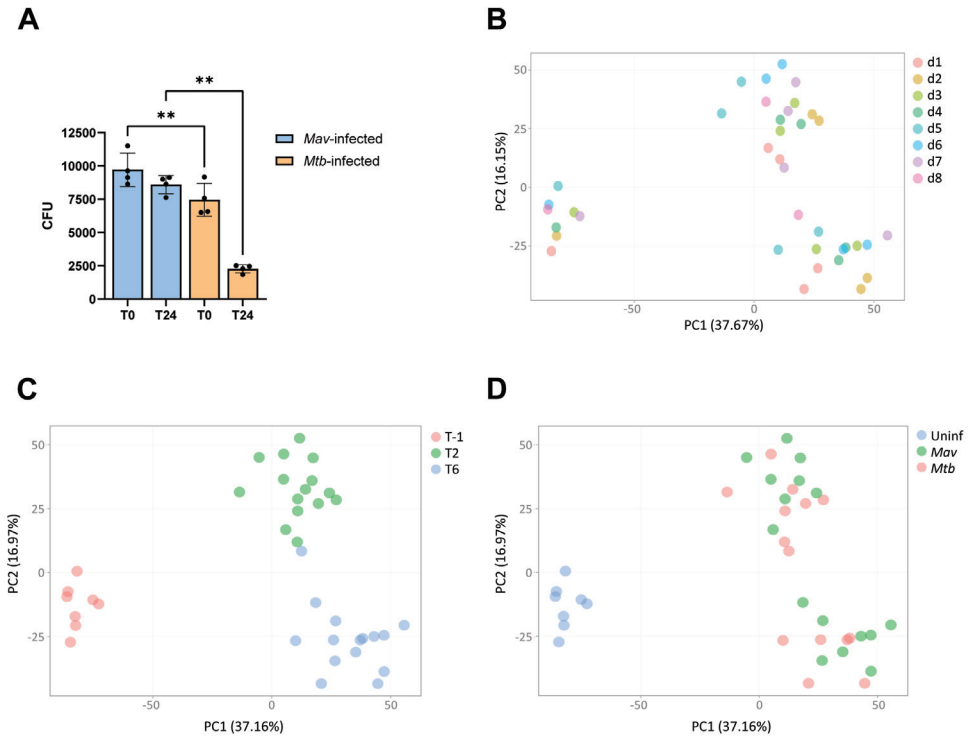

Figure 1. Transcriptome analysis of *Mav*- or *Mtb*-infected versus uninfected samples. **(A)** M2 macrophages were infected with either *Mav* or *Mtb* for 1 hour. After infection, cells were washed and lysed to determine the internalization (T0) and elimination of mycobacteria after 24 hours (T24). Dots represent the mean from triplicate wells of a single donor. Data represent the mean ± standard deviation (SD) from different donors (n=4). Differences were statistically significant by repeated measures one-way ANOVA with Šídák multiple comparison test. **p < 0.005. **(B-D)** The variance of the sequencing data from *Mav*- or *Mtb*-infected M2 macrophages from different donors (n=8 or n=7, respectively) and uninfected controls was described in PCA plots, illustrating separation by donor (B), timepoint (C), or infection status (D).

and upregulation of 241 and 907 genes after *Mav* infection (**Figure 2A, Supp Table 1**) or 248 and 872 genes after *Mtb* infection, respectively (**Figure 2B, Supp Table 1**). At 6 hours post-infection, the number of downregulated and upregulated genes were 734 and 1141 for *Mav* (**Figure 2C, Supp Table 1**), and 683 and 928 for *Mtb* (**Figure 2D, Supp Table 1**), respectively. To compare the similarity between DEGs in response to infection with either *Mav* or *Mtb*, we performed a Pearson correlation and Venn diagram analysis. The correlation in gene expression data derived from *Mav*- and *Mtb*-infected macrophages was very strong (Pearson correlation coefficients: 0.98 and 0.96 at 2 and 6 hours post-infection, respectively) (**Supp Figure 1A-B**), which was stronger than the correlation within each infection between the two timepoints (Pearson correlation coefficient: 0.83 and 0.84, for *Mav* and *Mtb* infection respectively) (**Supp Figure 1C-D**). Similarly, the Venn diagram analysis showed that the majority of the DEGs was affected by both mycobacteria compared to uninfected controls (**Figure 2E and F**).

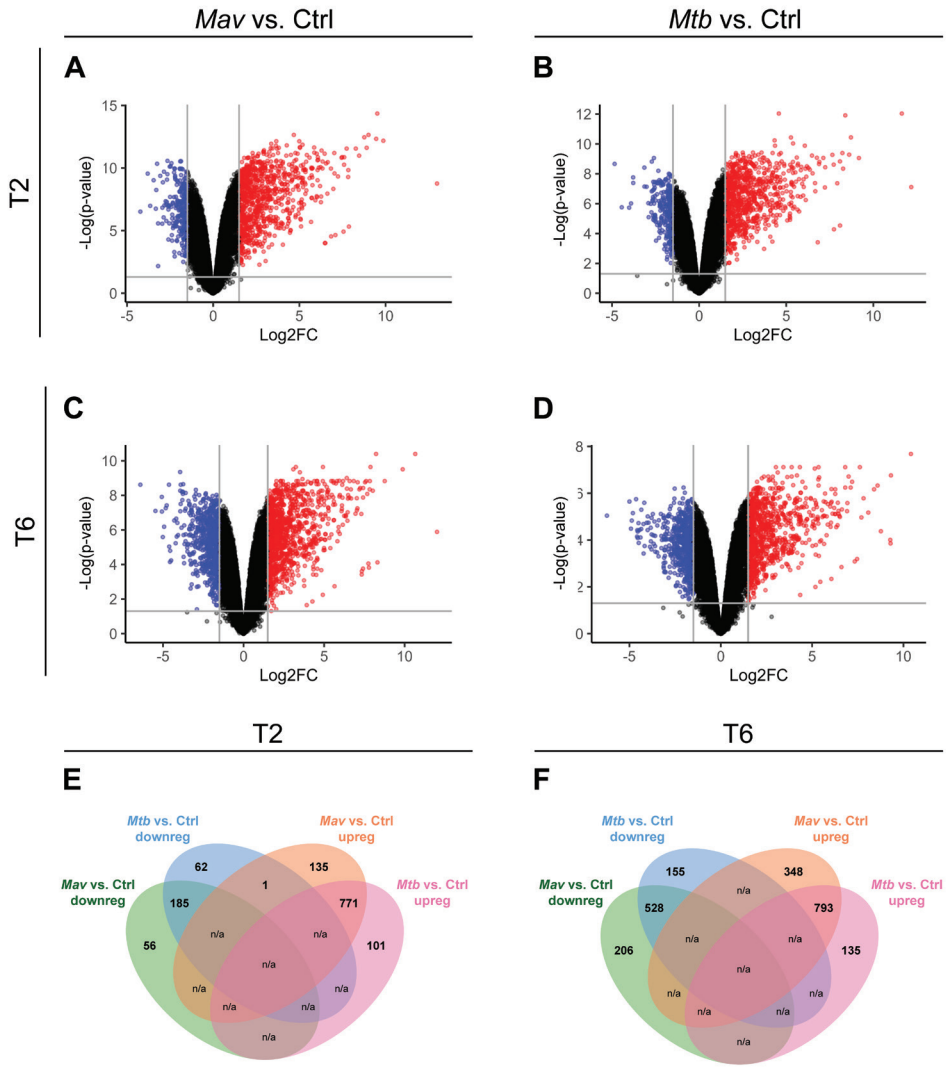

Figure 2. Differential expression analysis of primary human macrophages at 2 and 6 hours post-infection with *Mav* or *Mtb* compared to uninfected samples.
(A-D) Volcano plots showing DEGs among biological conditions of primary human macrophages at 2 (A-B) or 6 (C-D) hours post-infection with *Mav* (A-C) or *Mtb* (B-D) versus uninfected macrophages (Ctrl). Only log2 fold change (Log2FC) ≥ 1.5 or ≤ 1.5 and false discovery rate-adjusted p-values < 0.05 were analyzed. The upregulated genes are labelled red and downregulated genes are labelled blue. Non-differentially expressed genes are labeled black. **(E-F)** Venn diagram of the DEGs, showing the number of overlapping or unique down- or upregulated DEGs identified in macrophages at 2 (E) or 6 (F) hours post-infection infected with *Mav* or *Mtb* compared to the uninfected controls. N/A: comparison not applicable, as a gene cannot be down- and upregulated within the same infection and time point.

To assess the common host response against *Mav* and *Mtb*, DEGs shared after infection with both mycobacteria at either 2 or 6 hours post-infection were pooled, resulting in 610 downregulated genes and 1063 upregulated genes compared to uninfected

controls (**Supp Table 1**). Notably, one gene (FOS) was significantly upregulated by *Mav* and downregulated by *Mtb*. The 1673 DEGs shared by *Mav* and *Mtb* were subjected to Ingenuity Pathway Analysis (IPA) (**Supp table 1**). The top 20 pathways, enriched with 293 DEGs (17.5% of all DEGs), are shown in **Figure 3A**. These pathways were also among the highly ranked pathways in response to either *Mav* or *Mtb* compared to uninfected controls (**Supp Figure 2A-B**). The DEGs enriched in these top 20 pathways showed substantial overlap between pathways, predominantly in cytokines such as *IL1B*, *TNF*, *IL18*, *IL1A*, and *IL6*, as well as *NFKB1* and *NFKB2*. To comprehend the common host response, the overlapping network tool from IPA was used to identify clusters of related pathways. The analyses revealed two major nodes that were affected by both *Mav* and *Mtb* (**Figure 3B-C**). One node comprised pathways including Multiple Sclerosis Signaling Pathway, Role of Pattern Recognition Receptors in Recognition of Bacteria and Viruses, Pathogen Induced Cytokine Storm Signaling Pathway, Macrophage Classical Activation Signaling Pathway and NOD1/2 Signaling Pathway (**Figure 3B**). Gene Ontology (GO) Enrichment analysis with the 114 DEGs belonging to this node showed that most of the genes were associated with GO terms linked to a cytokine signaling response (**Figure 3D, Supp Figure 3A**), which, amongst others, included cytokines (i.e. *CXCL8*, *CSF2*, *IL36G*, *IL12B*, *IL15*, *IL10*, *CCL5* and *IL23A*), TNF superfamily ligands (*TNFSF10*, *TNFSF14*, *TNFSF15 and TNFSF9*) and Toll-like receptors (*TLR2*, *TLR3*, *TLR5* and *TLR6*) (**Figure 3E, Supp Table 1**).

The second node comprised pathways including Molecular Mechanisms of Cancer, Role of Macrophages, Fibroblasts and Endothelial Cells in Rheumatoid Arthritis, Role of Osteoblasts, Osteoclasts and Chondrocytes in Rheumatoid Arthritis, Hepatic Fibrosis Signaling Pathway, CDX Gastrointestinal Cancer Signaling Pathway, G-Protein Coupled Receptor Signaling and HMGB1 Signaling (**Figure 3C**). GO Enrichment analysis with 164 DEGs (excluding cytokines and cytokine receptors already discussed above) showed an association with mainly signal transduction by G protein-coupled receptor (GPCR) activity (**Figure 3F, Supp Figure 3B**). In total, the expression of 39 GPCRs was significantly affected by both *Mav* and *Mtb* (**Supp Table 1**). Based on the GPCR database (https://gpcrdb.org), a part of these GPCRs are involved in various signaling pathways with ligands including alicarboxylic acids (*HCAR2* and *HCAR3*) (27, 28), neurotransmitters (*CHRM3*), nucleotides (*ADORA2A*, *ADORA3* and *P2RY13*) (29-31), hormones (*SSTR2*, *OXTR*, *MAS1*, *MC1R* and *C5AR2*) (32-36) and Wnt ligands (*FZD2*, *FZD4*, *FZD6* and *LGR4*) (37). Finally, the biggest group comprised GPCRs involved in sensing lipids, including eicosanoids (*PTGIR*, *PTGER2*, *GPR31*, *CYSLTR1* and *CYSLTR2*), lysophospholipids (*LPAR5*, *LPAR6*, *GPR34*, *S1PR1*, *GPR65*, *GPR132* and *GPR82*), free fatty acids (*GPR84* and *FFAR4*) and sterols (*GPR183*) (**Figure 3G**). Taken together, these findings indicate that common changes in the host transcriptomic response upon infection with *Mav* and *Mtb* are characterized by an enhanced cytokine response and include regulation of GPCRs and likely concomitant lipid-mediated immunoregulation.

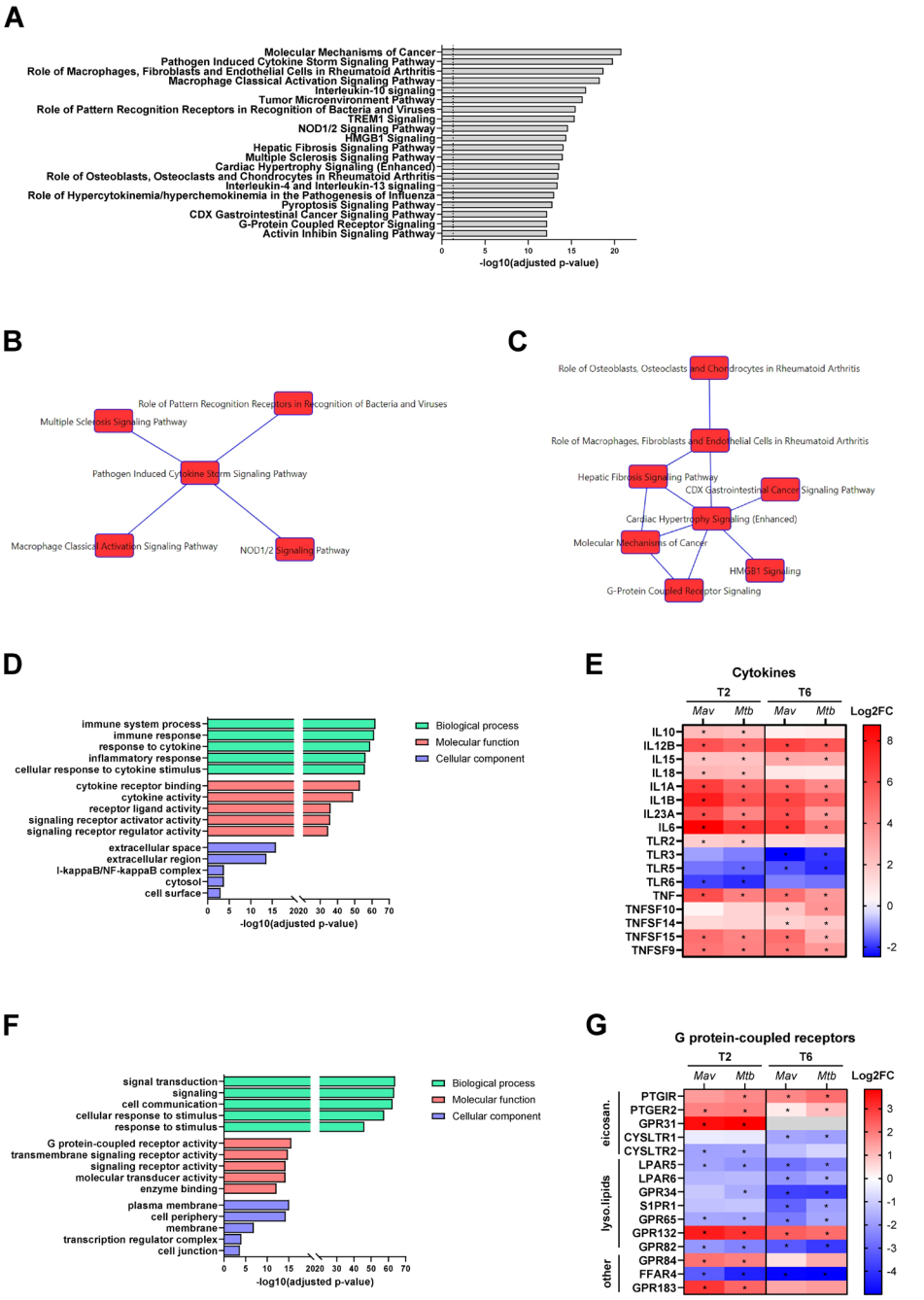

Figure 3. Enrichment analysis of DEGs shared by *Mav* and *Mtb* in primary human macrophages.
(A) The top 20 most significantly enriched IPA pathways of the 1673 commonly DEGs induced in macrophages infected with *Mav* and *Mtb* compared with uninfected controls. The enriched pathways were ranked by -log 10 p-value of gene enrichment. **(B-C)** Network analysis of enriched

pathways from A using IPA overlap networks tool. Links between indicated pathways indicates an overlap of minimum 30 DEGs. **(D)** GO enrichment analysis showing the top GO terms for biological process, molecular function and cellular component categories enriched for DEGs enriched in the pathways shown in B. The enriched ontology clusters were ranked by log10 p-value of gene enrichment. **(E)** Heatmap showing the expression patterns of various cytokines that were significantly affected by both *Mav* and *Mtb* infection at 2 (T2) and/or 6 (T6) hours post-infection, in comparison to uninfected controls. **(F)** GO enrichment analysis showing the top GO terms for biological process, molecular function and cellular component categories enriched for DEGs enriched in the pathways shown in C. The enriched ontology clusters were ranked by log10 p-value of gene enrichment. **(G)** Heatmap showing the expression patterns of lipid-binding GPCRs that were significantly affected by both *Mav* and *Mtb* infection at 2 (T2) and/or 6 (T6) hours post-infection, in comparison to uninfected controls. Grey box indicates no expression values could be determined. Ligands of genes are indicated with eicosan.: eicosanoids, lyso.lipids: lysophospholipids and other: free fatty acids and sterols.
Asterisk (*) indicates gene is differentially expressed in comparison to uninfected controls

Genes significantly regulated only by either *Mav* or *Mtb* indicate subtle, but not infection-specific, changes in host signaling pathways

To identify individual genes that were significantly regulated by either *Mav* or *Mtb*, DEGs from the two different timepoints were pooled. Although the correlation between host transcriptomic response to *Mav* and *Mtb* infection was notably high, genes were identified that were associated with either one of the infections (**Figure 2E and F**). In total, 561 genes were only differentially expressed by *Mav*, while 323 genes were only differentially regulated by *Mtb* (**Supp Table 1**). Pathway enrichment analysis revealed that the bone morphogenetic protein (BMP) signaling pathway (*BMP1*, *BMP2*, *JUN*, *MAPK8*, *RELA*, *SOS1*, *RAP1B* and *PRKAG2*), p75 neurotrophin receptor (NTR)-mediated signaling (*ARHGEF26*, *GNA13*, *ITSN1*, *MAPK8*, *PSEN2*, *RELA*, *SOS1* and *TIAM2*) and TNFR2 Signaling (*BIRC2*, *JUN*, *MAPK8* and *RELA*) were amongst the most enriched by *Mav* (**Figure 4A, Supp Table 1**). Importantly, these pathways were not specific for *Mav*, as they were also affected during *Mtb* infections (**Supp Figure 4**). GO Enrichment analysis with the 39 DEGs enriched in the top 10 pathways affected after *Mav* identified a potential more dominant role of phospholipases during *Mav* infection (**Figure 4B, Supp Table 1**). We observed that the expression of *NAPE-PLD* and *PLD6* (phospholipase D6) was significantly downregulated, while *PLCL1* (phospholipase C like 1) and PLD1 (phospholipase D1) were significantly upregulated by *Mav* and not by *Mtb* (**Figure 4C**). Interestingly, in response to both *Mav* and *Mtb*, we observed a significant downregulation of *FFAR4* (**Supp Table 1**), described to reduce lipid accumulation in macrophages (38). These observations suggest that host lipid metabolism is important for both mycobacteria, as well known for *Mtb* (39).

The genes that were significantly affected by *Mtb* were enriched in pathways associated with an immune response characterized by interferon-alpha/beta (*IFIT5*, *IFIT1*, *IFIT3*, *IRF4*, *ISG15*, *MX1*, and *MX2*) and interferon-gamma (*GBP3*, *IRF4*, *JAK2*, *OAS2*, *PTPN2*, and *TRIM5*) signaling pathways, as well as interferon-stimulated gene 15 (ISG15) signaling (*IFIT1*, *MX1*, *MX2*, *DTX3L*, *HERC5*, *IRF4*, *ISG15*, *ITGA2*, and *RIGI*) (**Figure 4D**). GO Enrichment analysis with the 29 DEGs enriched in the top 10 pathways after *Mtb* infection showed that these genes were associated with signaling in response to pathogens, consisting of mainly type I and type II interferon responses (**Figure 4E**). Like *Mtb*, *Mav* stimulated the expression of genes involved in interferon signaling (**Figure 4F**). This observation is reflected by the fact that these pathways were enriched among

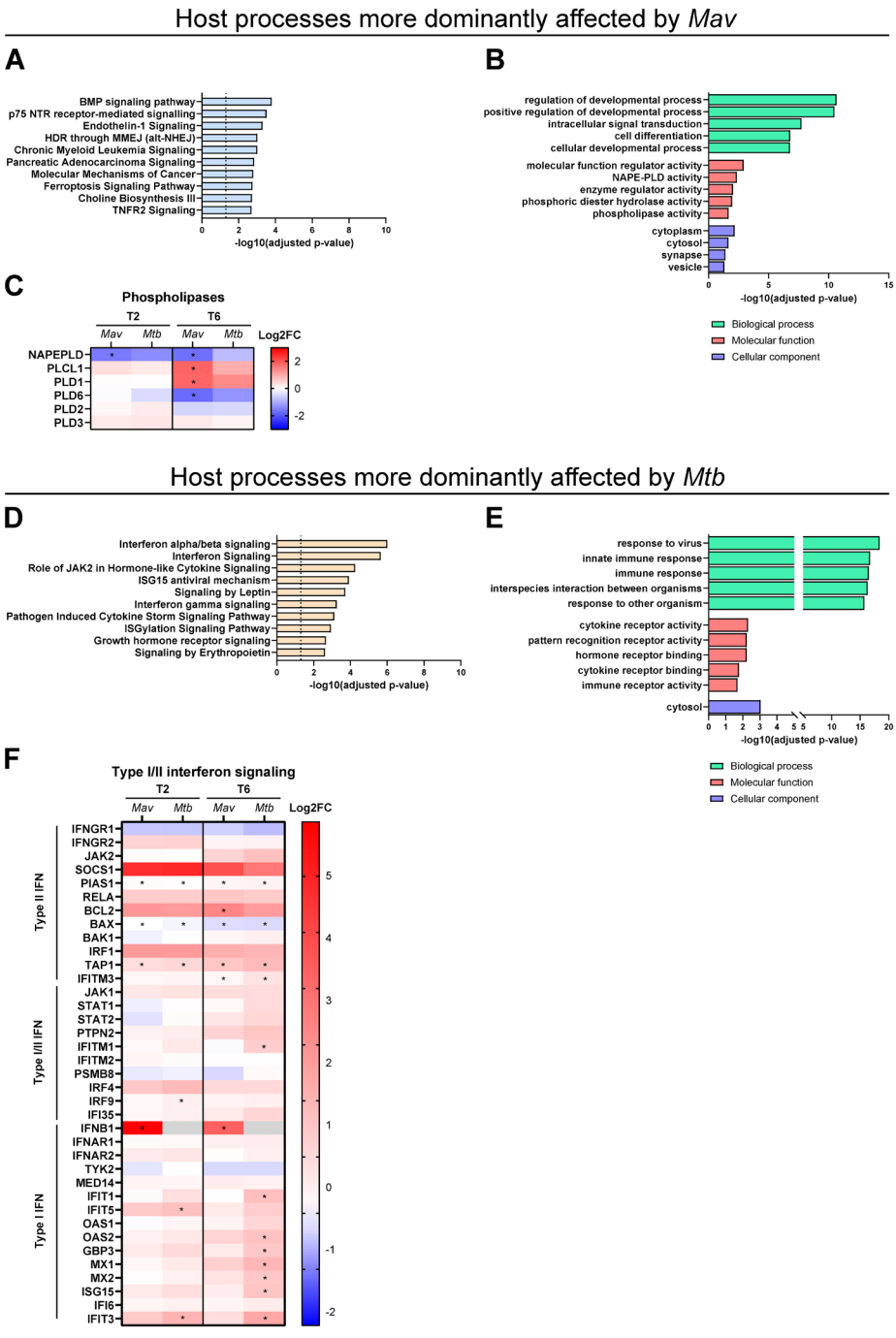

Figure 4. Genes significantly regulated only by either *Mav* or *Mtb* indicate subtle, but not infection-specific, changes in host signaling pathways

(A) The top 10 most significantly enriched IPA pathways of the 561 DEGs induced in exclusively *Mav*-

infected macrophages compared with uninfected controls. The enriched pathways were ranked by log 10 p-value of gene enrichment. **(B)** GO enrichment analysis showing the top GO terms for biological process, molecular function and cellular component categories enriched for DEGs enriched in the pathways shown in A. The enriched ontology clusters were ranked by log10 p-value of gene enrichment. **(C)** Heatmap showing the expression patterns of phospholipases that were exclusively induced by *Mav* infection at 2 (T2) and/or 6 (T6) hours post-infection, in comparison to uninfected controls, complemented with available expression data of phospholipases which were not affected by infection. Asterisk (*) indicates a DEG in comparison to uninfected controls. **(D)** The top 10 most significantly enriched IPA pathways of the 323 DEGs induced in exclusively *Mtb*-infected macrophages compared with uninfected controls. The enriched pathways were ranked by log 10 p-value of gene enrichment. **(E)** GO enrichment analysis showing the top GO terms for biological process, molecular function and cellular component categories enriched for DEGs enriched in the pathways shown in E. The enriched ontology clusters were ranked by log10 p-value of gene enrichment. **(F)** Heatmap showing the expression patterns of type I and II interferon signaling that were exclusively induced by *Mtb* infection 2 (T2) and/or 6 (T6) hours post-infection, in comparison to uninfected controls, complemented with available expression data of interferon genes which were not detected (grey). Asterisk (*) indicates a DEG in comparison to uninfected controls. Grey box indicates no expression values could be determined.

the transcriptomic response to both *Mav* and *Mtb* infections (**Supp Figure 4**). However, while *Mtb* evoked both type I and type II interferon signaling, *Mav* mainly affected type II interferon signaling. An exception was *IFNB1*, which was solely induced upon *Mav* infection.

Genes differentially expressed in macrophages infected with *Mav* compared to *Mtb* are associated with lipid metabolism, NGF-related apoptosis, and GIMAPs

In the previous analysis, we focused on the DEGs that were identified relative to uninfected controls. In the following analysis, the magnitude of gene expression was compared between the two infections to uncover significant changes between *Mav* and *Mtb* that may have been overlooked in comparison with uninfected controls. At 2 hours post-infection, this comparison revealed 14 genes that were significantly upregulated by *Mav* compared to *Mtb* and no genes that were downregulated in *Mav* (**Figure 5A, Table 1, Supp Table 1 and Supp Table 2**). At 6 hours post-infection, *Mav* infection resulted in 13 DEGs with downregulated expression levels and 17 DEGs with significantly upregulated expression levels compared to *Mtb* infection (**Figure 5B, Table 1, Supp Table 1 and Supp Table 2**). Protein-protein interaction (PPI) network analysis using the Search Tool for the Retrieval of Interacting Genes (STRING) database identified three distinct interaction networks including 24 of 38 genes: transcription regulators, GIMAPs, and cytokines (**Figure 5C**). Interestingly, among the genes that were not associated with a network, *FFAR2* and *GPR65* are related to lipid binding and/or metabolism and were significantly higher expressed in *Mav*-infected macrophages compared to those infected with *Mtb* (**Supp Table 2**) (40-42).

The first network consisted of *FOS*, *FOSB* (AP-1 transcription factor complex), *EGR1*, *EGR4* (EGR family of transcription factors), and ARC, which were all found to increase after *Mav* infection relative to *Mtb* infection (**Table 1**). *EGR1*, *EGR4*, *FOS*, and *FOSB* play key roles in regulating various biological processes including cell proliferation, differentiation and survival, and the production of pro-inflammatory cytokines (43). Furthermore, *EGR1*, *EGR4*, *FOS*, and *FOSB* are part of the Reactome pathway of nerve growth factor (NGF)-stimulated transcription (R-HSA-9031628).

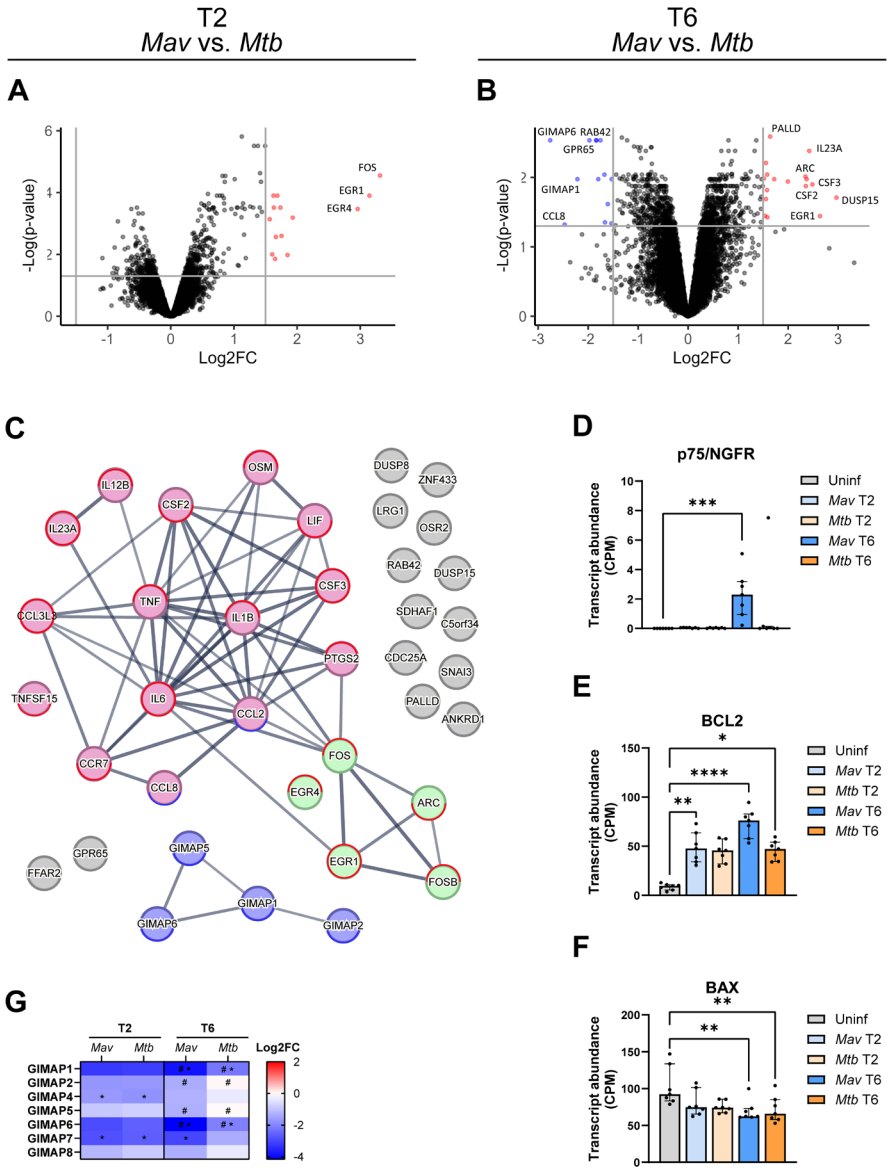

Figure 5. Genes differentially expressed in macrophages infected with *Mav* compared to *Mtb*.
(A-B) Volcano plots showing DEGs among biological conditions of primary human macrophages at 2 (A) or 6 (B) hours post-infection with *Mav* versus *Mtb* (n=7). Only log2 fold change (Log2FC) ≥ 1.5 or ≤ 1.5 and false discovery rate-adjusted p-values < 0.05 were analyzed. The upregulated genes are labelled red and downregulated genes are labelled blue. Non-differentially expressed genes are labeled black. **(C)** PPI network showing the DEGs from *Mav*-infected macrophages compared with *Mtb*-infected macrophages from A-B. The color representation indicates three distinct networks. Outline of genes indicate expression is increased (red) or decreased (blue), at 2 hours (upper circle) or 6 hours (lower circle), or both timepoints (full circle), post-infection with *Mav* compared to *Mtb* infection. **(D-F)** Transcript levels (count per million; CPM) of NGFR

(D), BLC2 (E) and BAX (F) in uninfected (grey), and *Mav* (blue shaded)- and *Mtb* (orange shaded)-infected macrophages at 2 and 6 hours post-infection. Differences were statistically significant by a Friedman test with Dunn's multiple comparison test. *p < 0.05, **p < 0.005, ***p < 0.001 and ****p < 0.0001. **(G)** Heatmap showing the expression patterns of GIMAPs that were differentially regulated in *Mav*-infected macrophages at 2 (T2) and/or 6 (T6) hours post-infection, compared to uninfected or *Mtb*-infected macrophages, complemented with available expression data of GIMAPs which were not affected by infection. Asterisk (*) indicates differential expression when compared to uninfected controls, whereas number sign (#) indicates differential expression between *Mav* and *Mtb*.

Previously, NGF-induced EGR1 downstream signaling involved *ARC*, which was also found to be significantly upregulated 6 hours post-infection with *Mav* compared to *Mtb* (**Table 1**) (44). NGF signaling involves a high-affinity receptor, TrkA, and a low-affinity receptor, p75/NGFR, which upon activation can induce either cell survival or apoptosis, respectively (45, 46). Interestingly, while no transcription of the TrkA receptor was detected in macrophages, the expression of the p75/*NGFR* gene as well as its signaling pathway were significantly upregulated 6 hours post-infection with *Mav* (**Figure 4A and 5D**). The expression of apoptosis-related genes showed significant upregulation of anti-apoptotic *BCL2*, while pro-apoptotic *BAX* was significantly downregulated in macrophages infected with *Mav* and *Mtb* (**Figure 5E-F**). Hence, these expression patterns indicate a reduced tendency of both *Mav*- and *Mtb*-infected host cells to undergo apoptosis, while the indicative pro-apoptotic p75 NTR pathway is also upregulated by *Mav*.

The second network consisted of genes of the GTPase of immunity-associated protein (GIMAP) family, which were significantly downregulated in macrophages infected with *Mav* compared to those infected with *Mtb*. *GIMAP1* and *GIMAP6* showed reduced expression in macrophages 6 hours post-infection with *Mav* and *Mtb* compared to uninfected controls, with significantly more silencing by *Mav* compared to *Mtb*. Although *GIMAP5* and *GIMAP2* were not significantly affected by mycobacterial infection when compared to uninfected controls, these genes were downregulated in macrophages infected with *Mav* compared to *Mtb*. Furthermore, while not differentially regulated between the two mycobacteria, *GIMAP4* and *GIMAP7* were significantly silenced by both *Mav* and *Mtb* 2 hours post-infection in comparison to uninfected controls.

Finally, the third PPI network consisted of genes encoding mainly cytokines. While we observed that both *Mav* and *Mtb* triggered significant early cytokine responses in macrophages compared to noninfected controls, *Mav* induced a more pronounced upregulation of several cytokines compared to *Mtb*. At 2 hours post-infection, these cytokines included *IL23A*, *IL6*, *IL1B*, *IL12B*, *CCL3L3*, *TNF* and *CSF3* (Table 1). At 6 hours post-infection, the upregulation of I*L23A*, *IL6*, *CCL3L3*, and *CSF3* persisted, along with the downregulation of *CCL8* and *CCL2* and additional upregulation of cytokines *TNFSF15*, *CSF2*, and *CCR7* in response to *Mav* compared to *Mtb* (**Table 1, Figure 5C**). The heightened expression of these molecules in response to *Mav* suggests this infection might be stimulating a more intense or swifter activation of immune pathways compared to *Mtb*. In addition, macrophages infected with *Mav* or *Mtb* showed increased expression of *PTGS2*, which was significantly higher upon *Mav* compared to *Mtb* infection.

Table 1. Genes, belonging to one of the STRING nodes, differentially modulated in primary human macrophages in response to *Mav* compared to *Mtb*.

Genes differentially expressed between *Mav* and *Mtb*				
2 hours post-infection			**DEG vs. uninfected**	
Gene	**Log2FC (*Mav* vs. *Mtb*)**	**p-value (adj)**	***Mav***	***Mtb***
Cytokines/Chemokines				
IL23A	1,85	1,05E-02	Up	Up
IL6	1,75	2,52E-03	Up	Up
OSM	1,74	3,06E-04	Up	-
IL1B	1,69	1,26E-04	Up	Up
IL12B	1,65	1,40E-02	Up	Up
CCL3L3	1,63	3,06E-04	Up	Up
TNF	1,62	1,26E-04	Up	Up
CSF3	1,57	7,26E-04	Up	Up
Transcription regulators				
FOS	3,31	2,80E-05	Up	Down
EGR1	3,14	1,26E-04	Up	-
EGR4	2,96	3,39E-04	Up	-
FOSB	1,93	6,47E-04	Up	-
Other				
PTGS2	1,66	2,72E-03	Up	Up
6 hours post-infection			**DEG vs. uninfected**	
Gene	**Log2FC (*Mav* vs. *Mtb*)**	**p-value (adj)**	***Mav***	***Mtb***
GIMAPs				
GIMAP1	-2,21	1,06E-02	Down	Down
GIMAP2	-1,66	4,45E-02	-	-
GIMAP5	-1,80	1,06E-02	-	-
GIMAP6	-2,76	2,93E-03	Down	Down
Cytokines/Chemokines				
CCL8	-2,47	4,79E-02	-	Up
CCL2	-1,67	9,12E-03	-	-
CSF3	2,49	1,26E-02	Up	Up
IL23A	2,42	4,15E-03	Up	Up
TNFSF15	2,35	1,33E-02	Up	Up
CSF2	2,35	9,73E-03	Up	Up
IL6	1,99	1,15E-02	Up	Up
CCL3L3	1,58	1,52E-02	Up	Up
CCR7	1,56	2,05E-02	Up	Up
LIF	1,52	9,98E-03	Up	Up
Transcription regulators				
EGR1	2,64	3,61E-02	-	Down
Other				
ARC	2,37	1,06E-02	Up	-

Taken together, macrophages infected with *Mav* showed upregulation of transcription factors related to NGF signaling and pro-inflammatory cytokines compared to *Mtb* infection, whereas GIMAPs were downregulated.

Validation of upregulated cytokine expression by assessing cytokine secretion by *Mav*- and *Mtb*-infected macrophages

To validate the transcriptome analysis results of cytokine production (**Supp Figure 5A**), secretion of a number of DEGs encoding cytokines in the supernatants of macrophages infected with *Mav* or *Mtb* 24 hours post-infection was measured using the Luminex assay. Compared to uninfected controls, both *Mav* and *Mtb* infection resulted in the induction of IL-6, IL-1β, TNF, IFN-γ, and to a lesser extent IL-12B and IFN-α2 (**Figure 6**). Induction of CSF2 and CSF3 by *Mav* or *Mtb* was not evident. Moreover, the transcriptome analysis between *Mav*- and *Mtb*-infected macrophages indicated the higher expression of certain cytokines after *Mav* infection (**Table 1, Supp Figure 5**). While *Mtb* rather than *Mav* appeared to induce higher levels of certain cytokines, no statistically significant differences in cytokine production were observed between *Mav* and *Mtb* infections (**Figure 6, Supp Figure 5**).

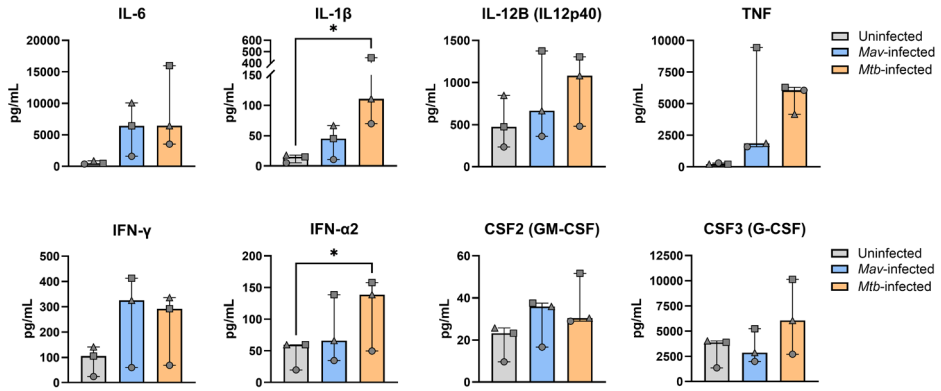

Figure 6. Cytokine production by *Mav*- and *Mtb*-infected macrophages.
Supernatants of *Mav*- and *Mtb* infected macrophages collected 24 hours post-infection were assessed for IL-6, IL-1β, IL-12B, TNF, IFN-γ, IFN-α2, CSF2 and CSF3 by the Luminex assay. Each symbol represents one donor (n=3) and data represent the median ± interquartile range. Statistical significance was tested using a Friedman test with Dunn's multiple comparisons test. *$p < 0.05$.

Discussion

There is a paucity of studies investigating the host-pathogen interactions and host transcriptomic response in *Mav*-infected primary human macrophages, cells crucial in immunity against *Mav* infection. Here, we report the first genome-wide transcriptome analysis of macrophages infected with *Mav*, and directly cross-reference these observations with *Mtb* infection. Our findings indicate that the transcriptional response to both infections largely overlaps, while some infection-specific responses are at play. The shared response to *Mav* and *Mtb* primarily involved cytokine signaling responses and GPCR signaling. In contrast, when comparing *Mav* and *Mtb* to one another and uninfected controls, differences were observed in the regulation of lipid metabolism, NGF-stimulated transcription, and the less-explored GIMAPS. Overall, we found alterations in the host response to both mycobacteria, providing insights into the shared and distinctive host processes that may play a role in the intracellular control of

Mav and *Mtb*, and which potentially offer targets for host-directed therapy.

Macrophages have a leading role in mycobacterial killing, antigen presentation, and directing immune responses. Cytokines like TNF, IL-1β, IL-6, and IL-10 produced by macrophages upon activation of pattern recognition receptors including Toll-like receptors (TLR) are crucial in bridging the innate and adaptive immune responses to mycobacterial infection (17). Consistent with previous findings, we observed a significant increase in pro-inflammatory cytokines (I*L12B*, *IL23A*, *TNF*, *IL1B*, *IL6*, *CCL20*, *CSF3*, and *CSF2*) in macrophages within hours of *Mav* or *Mtb* infection (25, 47, 48). Some of these cytokines in turn regulate TLR transcription to create feedback loops (49). We found increased *TLR2* expression and decreased *TLR5* expression in macrophages up to 6 hours post-infection with *Mav* and *Mtb*, as observed in prior studies (49, 50). In addition, *TLR3* and *TLR6* were downregulated in *Mav*- and *Mtb*-infected macrophages. Our cytokine secretion data validates that cytokine responses are a common feature of both *Mav* and *Mtb* infections. At 2 hours post-infection, however, differential expression analysis of infected macrophages showed a higher expression of pro-inflammatory cytokines such as *TNF*, *CSF3*, and *IL6* in response to *Mav* as compared to *Mtb*, which did not result in differences in cytokine secretion patterns between *Mav*- and *Mtb*-infected macrophages. Possibly, cytokine gene expression upon *Mtb* infection is slightly delayed as compared to *Mav* infection, which may be associated with the suggestion that mycobacterial virulence is inversely related to their ability to induce pro-inflammatory cytokines as an immune evasion strategy (51-53). Although *Mav* is considered less virulent than *Mtb*, we observed higher persistence of *Mav* in macrophages within 24 hours, suggesting that host cell antimycobacterial mechanisms other than cytokine production may be involved in the differential elimination of *Mav*.

Comparing the host transcriptomic response to *Mav* and *Mtb* revealed that both infections affected interferon signaling, which was more pronounced following *Mtb* infection. Both *Mav* and *Mtb* upregulated genes related to type II interferon (IFN) signaling. Interestingly, *Mav* affected type I IFN signaling only by upregulation of *IFNB1* (type I IFN), while *Mtb* induced the expression of genes downstream of type I IFN signaling (including *OAS2*, *MX1*, *MX2*, *ISG15*). In line with this, both *Mav* and *Mtb* seemed to induce secretion of IFN-γ to a similar extent, whereas secretion of IFN-α2 was slightly higher for *Mtb*-infected macrophages. While type II IFN (i.e. IFN-γ) is required for the resistance to mycobacteria, there is a lack of consensus on the role of type I IFNs in mycobacterial infections. In *Mav*-infected mice, continuous IFN-β infusion increased resistance, as evidenced by reduced bacterial loads (54). In contrast, type I IFN worsens *Mtb* infections (55), as shown by reduced bacterial loads in type I IFN receptor-deficient mice, and increased bacterial burden and pathology associated with recruitment of permissive macrophages via CCL2 when IFN-α/β was induced (56, 57). Remarkably, *CCL2* was more strongly downregulated in macrophages infected by *Mav* compared to *Mtb*. Moreover, type I IFN induces the immunosuppressive cytokine IL-10, and suppresses IL-1β production, resulting in the loss of protection against *Mtb* (58-60). *IL1B* was more strongly upregulated in *Mav*-infected cells compared to *Mtb* at 2 hours. IL-1β has a reciprocal control of type I IFN, by controlling type I IFN-induced accumulation of permissive macrophages at the site of infection through prostaglandin E2 (61). In line with the expression pattern of *IL1B*, *PTGS2*, which encodes for COX2 that mediates the production of prostaglandin E2, was more strongly upregulated by

Mav compared to *Mtb* at 2 hours. The disappearance of *IL1B* and *PTGS2* expression differences between *Mav* and *Mtb* at 6 hours post-infection may explain the comparable cytokine secretion observed following both infections. Taken together, IFN signaling was affected by both *Mav* and *Mtb* infection, with considerable variation over time.

The host transcriptomic regulation by *Mav* and *Mtb* infection also involved many genes linked to lipid metabolism, with some clear differences between both infections. Fatty acids are the most energy-dense substrates for energy production and are components of phospholipids in cell membranes (62). When nutrients are in excess, fatty acids can be stored as triglycerides, together with cholesteryl esters, in lipid droplets, which can be accessed via lipophagy (hydrolysis of lipid droplets by lipo-autophagosomes and lysosomes) or lipolysis (enzymatic hydrolysis of contents of cytosolic lipid droplets) during nutrient starvation (63). We found that infection with *Mav* and *Mtb* commonly upregulated *HCAR2* (promotes lipid accumulation associated with *Mtb* survival) (64), downregulated *FFAR4* (reduces lipid accumulation) (65), and upregulated *GPR156* (increases lipid accumulation) (66), indicating mycobacterial infection induces the accumulation and availability of lipids. Moreover, *Mav* and *Mtb* infections downregulated *GPR34* and closely related *GPR82* (both inhibit lipolysis) (67-70) and upregulated *GPR84*, *GPR132*, and *GPR183* (all three involved in sensing fatty acids or cholesterol) (71-75). In addition, expression of *FFAR2* (i.e. *GPR43*), associated with inhibition of lipolysis (40), varied in time, and was more strongly downregulated by *Mav* compared to *Mtb* infection. Lipid metabolism is known to be crucial for *Mtb* survival during infections; *Mtb* stimulates intracellular lipid accumulation and access to cytosolic lipids by escaping the phagosome or promoting the transport of lipid droplets to mycobacteria-containing vacuoles (39), creating a nutrient-rich environment that supports mycobacterial growth (76). While knowledge of the modulation of the host lipid metabolism during *Mav* infections is limited (77), our findings suggest that lipid metabolism is also essential during *Mav* infections. Indeed, there is a clear association between lower body fat mass and the development of *Mav*-LD (78, 79), and increased fatty acid metabolism has been linked to disease progression (76), indicating that altered lipid metabolism is also involved during *Mav* infection. This is supported by *Mav*-infected mice showing a correlation between increased fatty acid uptake and the formation of lipid-rich foamy macrophages with the progression of pulmonary disease (76). Notably, *Mav* but not *Mtb*, induced significant changes in the expression of phospholipases, which have a hydrolytic activity on host membrane phospholipids, resulting in the release of fatty acids for energy consumption, or anabolism of other lipids. These findings suggest that *Mav*, like *Mtb*, modulates lipid metabolism, possibly through different strategies in the battle between the host and mycobacteria for host lipids.

Another host pathway that was differentially regulated by *Mav* and *Mtb* is NGF signaling. Apoptosis of infected macrophages serves as an essential component of the host's defense mechanism against pathogens. Unlike necrosis, a type of cell death characterized by cell lysis releasing bacteria, apoptosis is a tightly regulated process that restricts bacterial growth and contributes to the activation of adaptive immunity (80). The role of apoptosis in both *Mav* and *Mtb* infection is debated, as inhibition of apoptosis is recognized as a key strategy to impair host immunity (81-84). However, mycobacteria can also benefit from the induction of apoptosis which enables them

to escape from dying cells to infect neighboring cells (85-87). Here, we observed that *Mav* infection induced expression of the neurotrophic factor receptor p75/*NGFR* 6 hours post-infection, which upon high or low affinity and activation by pro-NGF or NGF, respectively, is known to induce apoptosis in neurons (45, 46). Hence, macrophages infected with *Mav* rather than *Mtb* show a tendency towards induction of apoptosis, which is more likely to be induced during *Mav* infection compared to *Mtb* infection, which is supported by the finding that *Mtb* induced less apoptosis than other mycobacterial species including *Mav* (53). However, macrophages infected with *Mav* also showed increased expression of anti-apoptotic *BCL2*, while pro-apoptotic *BAX* was significantly silenced, as also seen in *Mtb*-infected cells, which promotes cell survival. Hence, during both *Mav* and *Mtb* infections, apoptosis may be inhibited, but macrophages upregulate NGF signaling only during *Mav* infection to promote apoptosis, resulting in differences in the cells' ability to induce apoptosis during *Mav* and *Mtb* infections.

Lastly, multiple GIMAPs were downregulated by both mycobacterial infections, and this downregulation was more pronounced during *Mav* infections. *GIMAP4* and *GIMAP7* were comparably silenced in macrophages by both *Mav* and *Mtb* 2 hours post-infection. At 6 hours post-infection, however, *Mav* showed a stronger suppression of *GIMAP1*, *GIMAP2*, *GIMAP5*, and *GIMAP6* expression compared to *Mtb*. To our knowledge, this is the first report of the differential expression of GIMAPs in human macrophages infected with mycobacteria. While the role of these proteins has mainly been described for the maintenance of lymphocytes (88-90), GIMAPs are also thought to be important in intracellular trafficking, as well as autophagy and lysosome function (91, 92), processes considered important in immune defenses against mycobacteria. GIMAP2 is found on lipid droplets to which it recruits GIMAP7, suggesting a role for these GIMAPs in lipid droplet trafficking (93). Furthermore, mutations in GIMAP5, which resides on lysosomes, are linked to increased autoimmune susceptibility (88), but its function in macrophages remains to be determined. GIMAP6 is involved in regulating efficient autophagy and facilitates antibacterial innate immunity by binding to and clearing pathogens (88, 92, 94). Finally, *GIMAP6* was downregulated in cattle infected with *Mav* subspecies paratuberculosis, while its role in disease susceptibility remains unknown (95). Taken together, while it remains unclear what the exact roles of GIMAPs are during mycobacterial infection, the more profoundly reduced expression of these proteins observed upon *Mav* infection may indicate a stronger impairment of the macrophage's ability to manage the infection. More investigation into the role of GIMAPs during mycobacterial infection is desired and may reveal novel targets for HDT.

This study has several limitations that should be considered. Firstly, as a validation strategy, cytokine regulation was assessed by a Luminex, but other differences found in the transcriptomic data were not validated further by complementary analyses. Hence, the findings from this study require further validation. Secondly, the analysis focused exclusively on early time points post-infection, which represents only a snapshot of macrophage activity shortly after infection and may not reflect the longer-term dynamic regulation of macrophage functions. Insufficient RNA yields at later time points (24 hours post-infection) unfortunately limited our ability to assess gene expression over a prolonged time course. Despite these limitations, a strength of this study was the use of RNA-seq, which, unlike microarray studies performed previously on *Mav*-infected cells (23-26), offers significant advantages including unbiased, genome-wide transcriptome

profiling of host gene expression without requiring pre-existing genome sequence information. Additionally, our study directly compares *Mav* and *Mtb* infections across primary human macrophages from matched donors, providing relevant insights into the differential responses of macrophages to these two mycobacterial infections. This direct comparison between *Mav* and *Mtb* facilitates extrapolation of shared findings given the wealth of studies that have functionally validated RNA regulation by *Mtb*.

In conclusion, this study on the host transcriptomic regulation of the human macrophage response to *Mav* and *Mtb* infection reveals a significant overlap between these infections in gene expression patterns. However, also distinct effects were observed in macrophage gene expression, being particularly pronounced during *Mav* infection. The functional implications of these expression patterns remain to be determined, in which our results provide direction to further explore host-pathogen interactions during *Mav* and *Mtb* infections.

Materials and methods

Cell culture

Buffy coats were collected from healthy anonymous Dutch adult donors after written informed consent (Sanquin Blood Bank, Amsterdam, the Netherlands). Primary human macrophages were obtained as previously described (96). In short, CD14+ monocytes were isolated from peripheral blood mononuclear cells using density gradient centrifugation with Ficoll (Pharmacy, LUMC, the Netherlands) and subsequently magnetic-activated cell sorting (MACS) with anti-CD14-coated microbeads (Miltenyi Biotec, Auburn, CA, USA). Purified CD14+ monocytes were cultured for 6 days at 37°C/5% CO_2 in Gibco Dutch modified Roswell Park Memorial Institute (RPMI) 1640 medium (ThermoFisher Scientific, Landsmeer, the Netherlands) supplemented with 10% fetal calf serum (FCS), 2 mM L-glutamine (PAA, Linz, Austria), 100 units/mL penicillin, 100 µg/mL streptomycin, and 50 ng/mL macrophage colony-stimulating factor (M-CSF, R&D Systems, Abingdon, UK) for anti-inflammatory M2 macrophage differentiation. Cytokines were refreshed at day 3 of differentiation. One day prior to experiments, macrophages were harvested and seeded into flat-bottom 96-well plates (30,000 cells/well), if not indicated otherwise, in complete RPMI medium without antibiotics or cytokines. Macrophage differentiation was validated based on cell surface marker expression (anti-human CD163-PE, CD14-PE-Cy7, and CD1a-Alexa Fluor 647 (1:20) from Biolegend (Amsterdam, the Netherlands) and anti-human CD11b-BB515 (1:20) from BD Biosciences) using flow cytometry and secretion of cytokines (IL-10 and IL-12) following 24 hours stimulation of cells with 100 ng/mL lipopolysaccharide (InvivoGen, San Diego, United States) using ELISA.

Bacterial cultures

Mav-Wasabi (laboratory strain 101) and *Mtb*-Venus (H37Rv) were cultured as described before (96, 97). Prior to experiments, bacterial concentrations were determined by measuring the optical density at 600 nm (OD_{600}).

Bacterial infection of cells

One day before infection, *Mav* and *Mtb* cultures were diluted to a density corresponding with early log-phase growth, OD_{600} of 0.25. On the day of macrophage infection, bacterial suspensions were diluted in antibiotic-free cell culture medium to consistently infect

cells with a multiplicity of infection (MOI) of 10. The accuracy of the MOI was verified using a standard CFU assay. Following inoculation of the cells, plates were centrifuged for 3 minutes at 130 rcf and incubated for 1 hour at 37°C/5% CO2. Cells were then treated with cell culture medium supplemented with 30 µg/mL gentamicin for 10 min to inactivate and remove residual extracellular bacteria, after which the medium was refreshed with medium containing 5 µg/mL gentamicin sulfate before cells were incubated at 37°C/5% CO_2 until indicated timepoints. Following incubation, supernatants were either stored at -20°C for Luminex assay or discarded, and cells were lysed using 100 µL of lysis buffer (H2O + 0.05% SDS) for the determination of intracellular bacterial burden using a CFU assay or lysed for RNA extraction as described below.

RNA isolation and sequencing

Total RNA was extracted from *Mav*- or *Mtb* infected macrophages seeded in a flat bottom 6-wells plate (900,000 cells/well) with 350 uL TRIzol™ reagent (Thermo Fisher Scientific) and using the Direct-zol RNA miniPrep kit (Zymo Research, Leiden, Netherlands) according to the manufacturer's protocol. Samples were diluted in 25 µL RNA-free water and the total RNA concentration of each sample was quantified using DeNovix DS-11 Spectrophotometer (ThermoFisher Scientific). Nanodrop (ThermoFisher Scientific) was used to determine RNA purity. Gene expressions were profiled using the NovaSeq 6000 platform (Illumina, San Diego, CA, USA) by GenomeScan (Leiden, Netherlands).

Data processing and analysis

RNA-Seq files were processed using the opensource BIOWDL RNAseq pipeline v5.0.0 (https://zenodo.org/record/5109461#.Ya2yLFPMJhE) developed at the LUMC. This pipeline performs FASTQ preprocessing (including quality control, quality trimming, and adapter clipping), RNA-Seq alignment, read quantification, and optionally transcript assembly. FastQC was used for checking raw read QC. Adapter clipping was performed using Cutadapt (v2.10) with default settings and standard illumina universal adapter "AGATCGGAAGAG". RNA-Seq reads' alignment was performed using STAR (v2.7.5a) on GRCh38 human reference genome. umi_tools (v1.1.1) was used to remove PCR duplicates detected with UMIs. The gene read quantification was performed using HTSeq-count (v0.12.4) with setting "–stranded=reverse". The gene annotation used for quantification was Ensembl version 111. Using the gene read count matrix, CPM was calculated per sample on all annotated genes. Genes with a higher log2CPM than 1 in at least 25% of all samples are kept for downstream analysis.

For the differential gene expression analysis and PCA plot creation, dgeAnalysis R-shiny application (https://github.com/LUMC/dgeAnalysis/tree/v1.4.4) was used. EdgeR (v3.34.1) with TMM normalization was used to perform differential gene expression analysis using donor as covariate. Genes with log2(fold change) ≥ 1.5 or ≤ -1.5 and Benjamini and Hochberg false discovery rate (FDR) adjusted p-values < 0.05 were designated as differentially expressed genes (DEGs).

Functional enrichment analysis

To classify the functions of the DEGs, functional enrichment analysis and clustering of biological pathways was performed through the use of QIAGEN Ingenuity Pathway Analysis (IPA) (QIAGEN Inc., https://digitalinsights.qiagen.com/IPA) (98). In addition, enrichment of Gene Ontology (GO) categories biological process, cellular component

and molecular function was analysed. Enrichment with an adjusted P value of < 0.05 was considered significantThe protein-protein interaction (PPI) networks of DEGs were predicted using the Search Tool for the Retrieval of Interacting Genes (STRING) database.

Cytokine secretion

Collected supernatants of uninfected or *Mav*- and *Mtb*-infected macrophages were filtered in FiltrEX 96-wells filter plates (Corning Costar) with pore size 0.2 µm to remove bacteria. The concentration of IL-6, IL-1β, TNF, IFN-γ, IL-12B, IFN-α2, CSF2, and CSF3 was measured by diluting the supernatants 4 times with Luminex Assay buffer (Bio-Rad, Hercules, CA, USA). Next, the Bio-Plex Pro Human Cytokine 48-plex Assay (Bio-Rad) was performed according to the manufacturer's instructions. Samples were measured on a Bio-Plex 200 System (Bio-Rad). Per analyte, a lower and upper limit of detection was determined with standard curves. Concentrations measured below the assays' detection limit were set to 1 pg/mL, and those measured over the detection limit were set to the maximum quantifiable pg/mL per analyte.

References

1. Ingen Jv, Wagner D, Gallagher J, Morimoto K, Lange C, Haworth CS, et al. Poor adherence to management guidelines in nontuberculous mycobacterial pulmonary diseases. Eur Respir J. 2017;49(2):1601855.
2. Prevots DR, Marras TK. Epidemiology of human pulmonary infection with nontuberculous mycobacteria: a review. Clin Chest Med. 2015;36(1):13-34.
3. van Ingen J, Obradovic M, Hassan M, Lesher B, Hart E, Chatterjee A, et al. Nontuberculous mycobacterial lung disease caused by Mycobacterium avium complex - disease burden, unmet needs, and advances in treatment developments. Expert Rev Resp Med. 2021;15(11):1387-401.
4. Namkoong H, Kurashima A, Morimoto K, Hoshino Y, Hasegawa N, Ato M, et al. Epidemiology of Pulmonary Nontuberculous Mycobacterial Disease, Japan. Emerg Infect Dis. 2016;22(6):1116-7.
5. Shah NM, Davidson JA, Anderson LF, Lalor MK, Kim J, Thomas HL, et al. Pulmonary Mycobacterium avium-intracellulare is the main driver of the rise in non-tuberculous mycobacteria incidence in England, Wales and Northern Ireland, 2007-2012. BMC Infect Dis. 2016;16:195.
6. Winthrop KL, Marras TK, Adjemian J, Zhang H, Wang P, Zhang Q. Incidence and Prevalence of Nontuberculous Mycobacterial Lung Disease in a Large U.S. Managed Care Health Plan, 2008-2015. Ann Am Thorac Soc. 2020;17(2):178-85.
7. Daley CL, Iaccarino JM, Lange C, Cambau E, Wallace RJ, Jr., Andrejak C, et al. Treatment of nontuberculous mycobacterial pulmonary disease: an official ATS/ERS/ESCMID/IDSA clinical practice guideline. Eur Respir J. 2020;56(1).
8. Griffith DE, Aksamit T, Brown-Elliott BA, Catanzaro A, Daley C, Gordin F, et al. An official ATS/IDSA statement: Diagnosis, treatment, and prevention of nontuberculous mycobacterial diseases. Am J Resp Crit Care. 2007;175(4):367-416.
9. Kwon YS, Koh WJ, Daley CL. Treatment of Mycobacterium avium Complex Pulmonary Disease. Tuberc Respir Dis (Seoul). 2019;82(1):15-26.
10. Xu HB, Jiang RH, Li L. Treatment outcomes for Mycobacterium avium complex: a systematic review and meta-analysis. Eur J Clin Microbiol Infect Dis. 2014;33(3):347-58.
11. Crowle AJ, Dahl R, Ross E, May MH. Evidence that vesicles containing living, virulent Mycobacterium tuberculosis or Mycobacterium avium in cultured human macrophages are not acidic. Infect Immun. 1991;59(5):1823-31.
12. Inderlied CB, Kemper CA, Bermudez LE. The Mycobacterium avium complex. Clin Microbiol Rev. 1993;6(3):266-310.
13. Lee H-J, Woo Y, Hahn T-W, Jung YM, Jung Y-J. Formation and Maturation of the Phagosome: A Key Mechanism in Innate Immunity against Intracellular Bacterial Infection. Microorganisms. 2020;8(9):1298.
14. Uribe-Querol E, Rosales C. Control of Phagocytosis by Microbial Pathogens. Front Immunol. 2017;8:1368.
15. Danelishvili L, Chinison JJJ, Pham T, Gupta R, Bermudez LE. The Voltage-Dependent Anion Channels (VDAC) of Mycobacterium avium phagosome are associated with bacterial survival and lipid export in macrophages. Scientific Reports. 2017;7(1):7007.

16. Danelishvili L, Bermudez LE. Mycobacterium avium *Mav*_2941 mimics phosphoinositol-3-kinase to interfere with macrophage phagosome maturation. Microbes Infect. 2015;17(9):628-37.
17. Park HE, Lee W, Choi S, Jung M, Shin MK, Shin SJ. Modulating macrophage function to reinforce host innate resistance against Mycobacterium avium complex infection. Front Immunol. 2022;13:931876.
18. Ottenhoff TH, Verreck FA, Lichtenauer-Kaligis EG, Hoeve MA, Sanal O, van Dissel JT. Genetics, cytokines and human infectious disease: lessons from weakly pathogenic mycobacteria and salmonellae. Nat Genet. 2002;32(1):97-105.
19. Blischak JD, Tailleux L, Mitrano A, Barreiro LB, Gilad Y. Mycobacterial infection induces a specific human innate immune response. Sci Rep. 2015;5:16882.
20. Lee J, Lee SG, Kim KK, Lim YJ, Choi JA, Cho SN, et al. Characterisation of genes differentially expressed in macrophages by virulent and attenuated Mycobacterium tuberculosis through RNA-Seq analysis. Sci Rep. 2019;9(1):4027.
21. Prombutara P, Adriansyah Putra Siregar T, Laopanupong T, Kanjanasirirat P, Khumpanied T, Borwornpinyo S, et al. Host cell transcriptomic response to the multidrug-resistant Mycobacterium tuberculosis clonal outbreak Beijing strain reveals its pathogenic features. Virulence. 2022;13(1):1810-26.
22. Pu W, Zhao C, Wazir J, Su Z, Niu M, Song S, et al. Comparative transcriptomic analysis of THP-1-derived macrophages infected with Mycobacterium tuberculosis H37Rv, H37Ra and BCG. J Cell Mol Med. 2021;25(22):10504-20.
23. Agdestein A, Jones A, Flatberg A, Johansen TB, Heffernan IA, Djonne B, et al. Intracellular growth of Mycobacterium avium subspecies and global transcriptional responses in human macrophages after infection. BMC Genomics. 2014;15:58.
24. Blumenthal A, Lauber J, Hoffmann R, Ernst M, Keller C, Buer J, et al. Common and unique gene expression signatures of human macrophages in response to four strains of Mycobacterium avium that differ in their growth and persistence characteristics. Infect Immun. 2005;73(6):3330-41.
25. Greenwell-Wild T, Vazquez N, Sim D, Schito M, Chatterjee D, Orenstein JM, et al. Mycobacterium avium infection and modulation of human macrophage gene expression. J Immunol. 2002;169(11):6286-97.
26. McGarvey JA, Wagner D, Bermudez LE. Differential gene expression in mononuclear phagocytes infected with pathogenic and non-pathogenic mycobacteria. Clin Exp Immunol. 2004;136(3):490-500.
27. Peters A, Rabe P, Liebing AD, Krumbholz P, Nordstrom A, Jager E, et al. Hydroxycarboxylic acid receptor 3 and GPR84 - Two metabolite-sensing G protein-coupled receptors with opposing functions in innate immune cells. Pharmacol Res. 2022;176:106047.
28. Zandi-Nejad K, Takakura A, Jurewicz M, Chandraker AK, Offermanns S, Mount D, et al. The role of HCA2 (GPR109A) in regulating macrophage function. FASEB J. 2013;27(11):4366-74.
29. Klaver D, Thurnher M. Control of Macrophage Inflammation by P2Y Purinergic Receptors. Cells. 2021;10(5).
30. Jacobson KA, Merighi S, Varani K, Borea PA, Baraldi S, Aghazadeh Tabrizi M, et al. A(3) Adenosine Receptors as Modulators of Inflammation: From Medicinal Chemistry to Therapy. Med Res Rev. 2018;38(4):1031-72.
31. Aggarwal NR, D'Alessio FR, Eto Y, Chau E, Avalos C, Waickman AT, et al. Macrophage A2A adenosinergic receptor modulates oxygen-induced augmentation of murine lung injury. Am J Respir Cell Mol Biol. 2013;48(5):635-46.
32. Li XX, Clark RJ, Woodruff TM. C5aR2 Activation Broadly Modulates the Signaling and Function of Primary Human Macrophages. J Immunol. 2020;205(4):1102-12.
33. Rinne P, Rami M, Nuutinen S, Santovito D, van der Vorst EPC, Guillamat-Prats R, et al. Melanocortin 1 Receptor Signaling Regulates Cholesterol Transport in Macrophages. Circulation. 2017;136(1):83-97.
34. Hammer A, Yang G, Friedrich J, Kovacs A, Lee DH, Grave K, et al. Role of the receptor Mas in macrophage-mediated inflammation in vivo. Proc Natl Acad Sci U S A. 2016;113(49):14109-14.
35. Szeto A, Sun-Suslow N, Mendez AJ, Hernandez RI, Wagner KV, McCabe PM. Regulation of the macrophage oxytocin receptor in response to inflammation. Am J Physiol Endocrinol Metab. 2017;312(3):E183-E9.
36. Elliott DE, Li J, Blum AM, Metwali A, Patel YC, Weinstock JV. SSTR2A is the dominant somatostatin receptor subtype expressed by inflammatory cells, is widely expressed and directly regulates T cell IFN-gamma release. Eur J Immunol. 1999;29(8):2454-63.
37. Schaale K, Neumann J, Schneider D, Ehlers S, Reiling N. Wnt signaling in macrophages: augmenting and inhibiting mycobacteria-induced inflammatory responses. Eur J Cell Biol. 2011;90(6-7):553-9.
38. Zhang LS, Zhang ZS, Wu YZ, Guo B, Li J, Huang XQ, et al. Activation of free fatty acid receptors, FFAR1 and FFAR4, ameliorates ulcerative colitis by promote fatty acid metabolism and mediate macrophage polarization. Int Immunopharmacol. 2024;130:111778.
39. van der Klugt T, van den Biggelaar R, Saris A. Host and bacterial lipid metabolism during tuberculosis infections: possibilities to synergise host- and bacteria-directed therapies. Crit Rev Microbiol. 2024:1-21.

40. Al Mahri S, Malik SS, Al Ibrahim M, Haji E, Dairi G, Mohammad S. Free Fatty Acid Receptors (FFARs) in Adipose: Physiological Role and Therapeutic Outlook. Cells. 2022;11(4).
41. Lin J, Liu Q, Zhang H, Huang X, Zhang R, Chen S, et al. C1q/Tumor necrosis factor-related protein-3 protects macrophages against LPS-induced lipid accumulation, inflammation and phenotype transition via PPARgamma and TLR4-mediated pathways. Oncotarget. 2017;8(47):82541-57.
42. Xu C, Sarver DC, Lei X, Sahagun A, Zhong J, Na CH, et al. CTRP6 promotes the macrophage inflammatory response, and its deficiency attenuates LPS-induced inflammation. J Biol Chem. 2024;300(1):105566.
43. Bahrami S, Drablos F. Gene regulation in the immediate-early response process. Adv Biol Regul. 2016;62:37-49.
44. Adams KW, Kletsov S, Lamm RJ, Elman JS, Mullenbrock S, Cooper GM. Role for Egr1 in the Transcriptional Program Associated with Neuronal Differentiation of PC12 Cells. PLoS One. 2017;12(1):e0170076.
45. Bruno F, Arcuri D, Vozzo F, Malvaso A, Montesanto A, Maletta R. Expression and Signaling Pathways of Nerve Growth Factor (NGF) and Pro-NGF in Breast Cancer: A Systematic Review. Curr Oncol. 2022;29(11):8103-20.
46. Dechant G, Barde YA. The neurotrophin receptor p75(NTR): novel functions and implications for diseases of the nervous system. Nat Neurosci. 2002;5(11):1131-6.
47. Casey ME, Meade KG, Nalpas NC, Taraktsoglou M, Browne JA, Killick KE, et al. Analysis of the Bovine Monocyte-Derived Macrophage Response to Mycobacterium avium Subspecies Paratuberculosis Infection Using RNA-seq. Front Immunol. 2015;6:23.
48. Kawka M, Plocinska R, Plocinski P, Pawelczyk J, Slomka M, Gatkowska J, et al. The functional response of human monocyte-derived macrophages to serum amyloid A and Mycobacterium tuberculosis infection. Front Immunol. 2023;14:1238132.
49. Wang T, Lafuse WP, Zwilling BS. Regulation of toll-like receptor 2 expression by macrophages following Mycobacterium avium infection. J Immunol. 2000;165(11):6308-13.
50. Ariel O, Gendron D, Dudemaine PL, Gevry N, Ibeagha-Awemu EM, Bissonnette N. Transcriptome Profiling of Bovine Macrophages Infected by Mycobacterium avium spp. paratuberculosis Depicts Foam Cell and Innate Immune Tolerance Phenotypes. Front Immunol. 2019;10:2874.
51. Strohmeier GR, Fenton MJ. Roles of lipoarabinomannan in the pathogenesis of tuberculosis. Microbes Infect. 1999;1(9):709-17.
52. Borrmann E, Mobius P, Diller R, Kohler H. Divergent cytokine responses of macrophages to Mycobacterium avium subsp. paratuberculosis strains of Types II and III in a standardized in vitro model. Vet Microbiol. 2011;152(1-2):101-11.
53. Feng Z, Bai X, Wang T, Garcia C, Bai A, Li L, et al. Differential Responses by Human Macrophages to Infection With Mycobacterium tuberculosis and Non-tuberculous Mycobacteria. Front Microbiol. 2020;11:116.
54. Denis M. Recombinant murine beta interferon enhances resistance of mice to systemic Mycobacterium avium infection. Infect Immun. 1991;59(5):1857-9.
55. Cooper AM, Mayer-Barber KD, Sher A. Role of innate cytokines in mycobacterial infection. Mucosal Immunol. 2011;4(3):252-60.
56. Antonelli LR, Gigliotti Rothfuchs A, Goncalves R, Roffe E, Cheever AW, Bafica A, et al. Intranasal Poly-IC treatment exacerbates tuberculosis in mice through the pulmonary recruitment of a pathogen-permissive monocyte/macrophage population. J Clin Invest. 2010;120(5):1674-82.
57. Sabir N, Hussain T, Shah SZA, Zhao D, Zhou X. IFN-beta: A Contentious Player in Host-Pathogen Interaction in Tuberculosis. Int J Mol Sci. 2017;18(12).
58. Novikov A, Cardone M, Thompson R, Shenderov K, Kirschman KD, Mayer-Barber KD, et al. Mycobacterium tuberculosis triggers host type I IFN signaling to regulate IL-1beta production in human macrophages. J Immunol. 2011;187(5):2540-7.
59. Mayer-Barber KD, Andrade BB, Barber DL, Hieny S, Feng CG, Caspar P, et al. Innate and adaptive interferons suppress IL-1alpha and IL-1beta production by distinct pulmonary myeloid subsets during Mycobacterium tuberculosis infection. Immunity. 2011;35(6):1023-34.
60. McNab FW, Ewbank J, Howes A, Moreira-Teixeira L, Martirosyan A, Ghilardi N, et al. Type I IFN induces IL-10 production in an IL-27-independent manner and blocks responsiveness to IFN-gamma for production of IL-12 and bacterial killing in Mycobacterium tuberculosis-infected macrophages. J Immunol. 2014;193(7):3600-12.
61. Mayer-Barber KD, Andrade BB, Oland SD, Amaral EP, Barber DL, Gonzales J, et al. Host-directed therapy of tuberculosis based on interleukin-1 and type I interferon crosstalk. Nature. 2014;511(7507):99-103.
62. Remmerie A, Scott CL. Macrophages and lipid metabolism. Cell Immunol. 2018;330:27-42.
63. Zechner R, Madeo F, Kratky D. Cytosolic lipolysis and lipophagy: two sides of the same coin. Nat

Rev Mol Cell Biol. 2017;18(11):671-84.
64. Naz F, Arish M. GPCRs as an emerging host-directed therapeutic target against mycobacterial infection: From notion to reality. Br J Pharmacol. 2022;179(21):4899-909.
65. Stuttgen GM, Sahoo D. FFAR4: A New Player in Cardiometabolic Disease? Endocrinology. 2021;162(8).
66. Kalam H, Chou CH, Kadoki M, Graham DB, Deguine J, Hung DT, et al. Identification of host regulators of Mycobacterium tuberculosis phenotypes uncovers a role for the MMGT1-GPR156 lipid droplet axis in persistence. Cell Host Microbe. 2023;31(6):978-92 e5.
67. Yasuda D, Hamano F, Masuda K, Dahlstrom M, Kobayashi D, Sato N, et al. Inverse agonism of lysophospholipids with cationic head groups at Gi-coupled receptor GPR82. Eur J Pharmacol. 2023;954:175893.
68. Engel KM, Schrock K, Teupser D, Holdt LM, Tonjes A, Kern M, et al. Reduced food intake and body weight in mice deficient for the G protein-coupled receptor GPR82. PLoS One. 2011;6(12):e29400.
69. Andreu N, Phelan J, de Sessions PF, Cliff JM, Clark TG, Hibberd ML. Primary macrophages and J774 cells respond differently to infection with Mycobacterium tuberculosis. Sci Rep. 2017;7:42225.
70. Liebscher I, Muller U, Teupser D, Engemaier E, Engel KM, Ritscher L, et al. Altered immune response in mice deficient for the G protein-coupled receptor GPR34. J Biol Chem. 2011;286(3):2101-10.
71. Wang J, Wu X, Simonavicius N, Tian H, Ling L. Medium-chain fatty acids as ligands for orphan G protein-coupled receptor GPR84. J Biol Chem. 2006;281(45):34457-64.
72. Hannedouche S, Zhang J, Yi T, Shen W, Nguyen D, Pereira JP, et al. Oxysterols direct immune cell migration via EBI2. Nature. 2011;475(7357):524-7.
73. Foster JR, Ueno S, Chen MX, Harvey J, Dowell SJ, Irving AJ, et al. N-Palmitoylglycine and other N-acylamides activate the lipid receptor G2A/GPR132. Pharmacol Res Perspect. 2019;7(6):e00542.
74. Foo CX, Bartlett S, Chew KY, Ngo MD, Bielefeldt-Ohmann H, Arachchige BJ, et al. GPR183 antagonism reduces macrophage infiltration in influenza and SARS-CoV-2 infection. Eur Respir J. 2023;61(3).
75. Recio C, Lucy D, Purvis GSD, Iveson P, Zeboudj L, Iqbal AJ, et al. Activation of the Immune-Metabolic Receptor GPR84 Enhances Inflammation and Phagocytosis in Macrophages. Front Immunol. 2018;9:1419.
76. Choi S, Lee JM, Kim KES, Park JH, Kim LH, Park J, et al. Protein-energy restriction-induced lipid metabolism disruption causes stable-to-progressive disease shift in Mycobacterium avium-infected female mice. EBioMedicine. 2024;105:105198.
77. Thirunavukkarasu S, de Silva K, Plain KM, R JW. Role of host- and pathogen-associated lipids in directing the immune response in mycobacterial infections, with emphasis on Mycobacterium avium subsp. paratuberculosis. Crit Rev Microbiol. 2016;42(2):262-75.
78. Kartalija M, Ovrutsky AR, Bryan CL, Pott GB, Fantuzzi G, Thomas J, et al. Patients with nontuberculous mycobacterial lung disease exhibit unique body and immune phenotypes. Am J Respir Crit Care Med. 2013;187(2):197-205.
79. Tasaka S, Hasegawa N, Nishimura T, Yamasawa W, Kamata H, Shinoda H, et al. Elevated serum adiponectin level in patients with Mycobacterium avium-intracellulare complex pulmonary disease. Respiration. 2010;79(5):383-7.
80. Behar SM, Martin CJ, Booty MG, Nishimura T, Zhao X, Gan HX, et al. Apoptosis is an innate defense function of macrophages against Mycobacterium tuberculosis. Mucosal Immunol. 2011;4(3):279-87.
81. Keane J, Shurtleff B, Kornfeld H. TNF-dependent BALB/c murine macrophage apoptosis following Mycobacterium tuberculosis infection inhibits bacillary growth in an IFN-gamma independent manner. Tuberculosis (Edinb). 2002;82(2-3):55-61.
82. Liu M, Li W, Xiang X, Xie J. Mycobacterium tuberculosis effectors interfering host apoptosis signaling. Apoptosis. 2015;20(7):883-91.
83. Bermudez LE, Danelishvili L, Babrack L, Pham T. Evidence for genes associated with the ability of Mycobacterium avium subsp. hominissuis to escape apoptotic macrophages. Front Cell Infect Microbiol. 2015;5:63.
84. Early J, Fischer K, Bermudez LE. Mycobacterium avium uses apoptotic macrophages as tools for spreading. Microb Pathog. 2011;50(2):132-9.
85. Augenstreich J, Arbues A, Simeone R, Haanappel E, Wegener A, Sayes F, et al. ESX-1 and phthiocerol dimycocerosates of Mycobacterium tuberculosis act in concert to cause phagosomal rupture and host cell apoptosis. Cell Microbiol. 2017;19(7).
86. Aguilo JI, Alonso H, Uranga S, Marinova D, Arbues A, de Martino A, et al. ESX-1-induced apoptosis is involved in cell-to-cell spread of Mycobacterium tuberculosis. Cell Microbiol. 2013;15(12):1994-2005.
87. Fratazzi C, Arbeit RD, Carini C, Remold HG. Programmed cell death of Mycobacterium avium serovar 4-infected human macrophages prevents the mycobacteria from spreading and induces mycobacterial growth inhibition by freshly added, uninfected macrophages. J Immunol. 1997;158(9):4320-7.
88. Pascall JC, Webb LMC, Eskelinen EL, Innocentin S, Attaf-Bouabdallah N, Butcher GW. GIMAP6 is

required for T cell maintenance and efficient autophagy in mice. PLoS One. 2018;13(5):e0196504.
89. Saunders A, Webb LM, Janas ML, Hutchings A, Pascall J, Carter C, et al. Putative GTPase GIMAP1 is critical for the development of mature B and T lymphocytes. Blood. 2010;115(16):3249-57.
90. Schnell S, Demolliere C, van den Berk P, Jacobs H. Gimap4 accelerates T-cell death. Blood. 2006;108(2):591-9.
91. Limoges MA, Cloutier M, Nandi M, Ilangumaran S, Ramanathan S. The GIMAP Family Proteins: An Incomplete Puzzle. Front Immunol. 2021;12:679739.
92. Yao Y, Du Jiang P, Chao BN, Cagdas D, Kubo S, Balasubramaniyam A, et al. GIMAP6 regulates autophagy, immune competence, and inflammation in mice and humans. J Exp Med. 2022;219(6).
93. Schwefel D, Frohlich C, Eichhorst J, Wiesner B, Behlke J, Aravind L, et al. Structural basis of oligomerization in septin-like GTPase of immunity-associated protein 2 (GIMAP2). Proc Natl Acad Sci U S A. 2010;107(47):20299-304.
94. Pascall JC, Rotondo S, Mukadam AS, Oxley D, Webster J, Walker SA, et al. The immune system GTPase GIMAP6 interacts with the Atg8 homologue GABARAPL2 and is recruited to autophagosomes. PLoS One. 2013;8(10):e77782.
95. Thirunavukkarasu S, Plain KM, de Silva K, Begg D, Whittington RJ, Purdie AC. Expression of genes associated with cholesterol and lipid metabolism identified as a novel pathway in the early pathogenesis of Mycobacterium avium subspecies paratuberculosis-infection in cattle. Vet Immunol Immunopathol. 2014;160(3-4):147-57.
96. Kilinc G, Walburg KV, Franken K, Valkenburg ML, Aubry A, Haks MC, et al. Development of Human Cell-Based In Vitro Infection Models to Determine the Intracellular Survival of Mycobacterium avium. Front Cell Infect Microbiol. 2022;12:872361.
97. Korbee CJ, Heemskerk MT, Kocev D, van Strijen E, Rabiee O, Franken K, et al. Combined chemical genetics and data-driven bioinformatics approach identifies receptor tyrosine kinase inhibitors as host-directed antimicrobials. Nat Commun. 2018;9(1):358.
98. Kramer A, Green J, Pollard J, Jr., Tugendreich S. Causal analysis approaches in Ingenuity Pathway Analysis. Bioinformatics. 2014;30(4):523–30.

Supplementary material

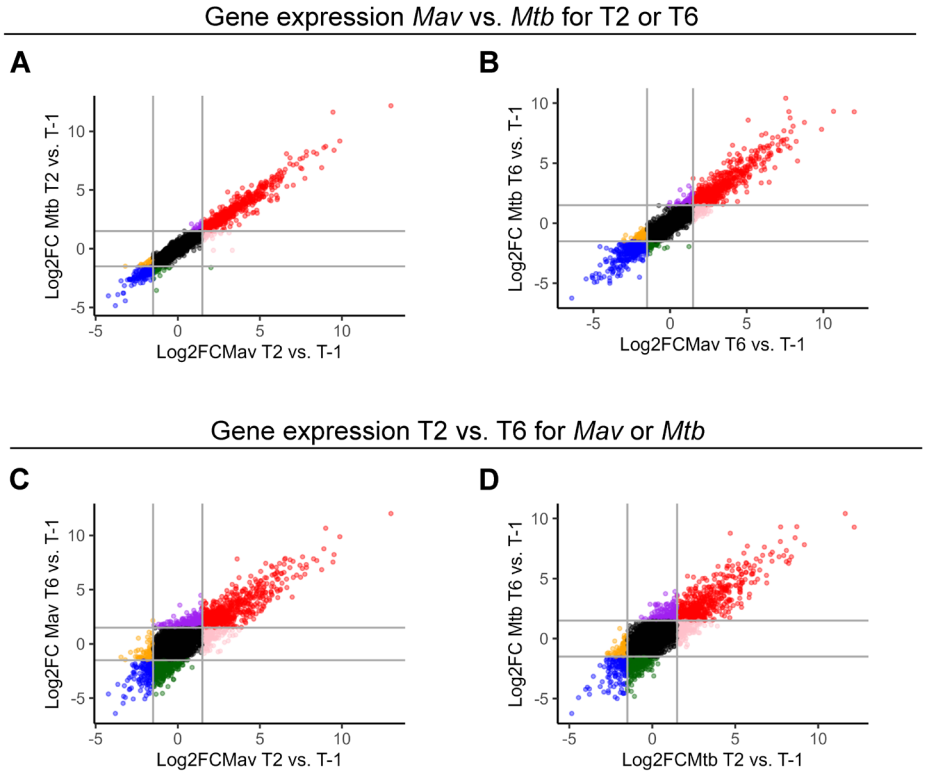

Supplementary Figure 1. Transcriptomic response of primary human macrophages infected with *Mav* or *Mtb* at 2 or 6 hours post-infection and uninfected controls.
(A-B) Scatterplot showing gene expression levels (Log2FC ≥ 1.5 or ≤ 1.5) of macrophages infected with *Mav* vs. *Mtb* at 2 hours (A) or 6 hours (B) post-infection compared to uninfected controls. Genes with Log2FC ≥ 1.5 and Log2FC ≤ 1.5 by both *Mav* and *Mtb* are expressed red and blue, respectively. **(C-D)** Scatterplot showing gene expression levels (Log2FC ≥ 1.5 or ≤ 1.5) of macrophages 2 hours vs. 6 hours post-infected with *Mav* (C) or *Mtb* (D) compared to uninfected controls. Genes with Log2FC ≥ 1.5 and Log2FC ≤ 1.5 by both timepoints post-infection are expressed red and blue, respectively.

Supplementary Table 1. Gene expression values of *Mav*- and *Mtb*-infected macrophages compared to uninfected controls.
Data will be made available on request from the authors.

Supplementary Table 2. Genes differentially expressed between *Mav* and *Mtb* not associated with a STRING-node.

Genes differentially expressed between *Mav* and *Mtb*				
2 hours post-infection			**DEG vs. uninfected**	
Gene	**Log2FC (*Mav* vs. *Mtb*)**	**p-value (adj)**	***Mav***	***Mtb***
OSR2	1,34	9,89E-03	Up	Up
6 hours post-infection			**DEG vs. uninfected**	
Gene	**Log2FC (*Mav* vs. *Mtb*)**	**p-value (adj)**	***Mav***	***Mtb***
GPR65	-1,98	2,93E-03	Down	Down
ENSG00000289424	-1,84	2,93E-03	Down	-
SNAI3	-1,84	2,93E-03	-	-
RAB42	-1,75	2,93E-03	Down	Down
FFAR2	-1,61	2,43E-02	-	Up
LRG1	-1,53	4,61E-02	-	Up
SDHAF1	-1,53	1,06E-02	Down	-
DUSP15	2,97	1,95E-02	Up	Up
CDC25A	1,72	1,06E-02	Up	-
PALLD	1,64	2,58E-03	Up	-
DUSP8	1,59	3,75E-02	Up	Up
ZNF433	1,58	9,12E-03	Up	-
ANKRD1	1,56	6,19E-03	Up	Up
C5orf34	1,54	3,58E-02	Up	-

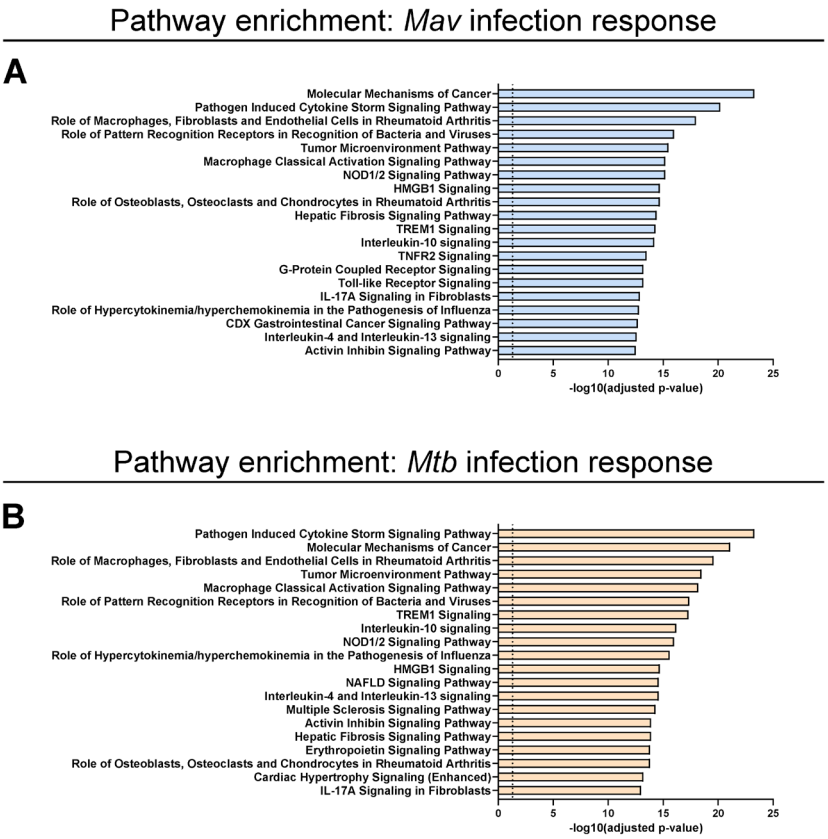

Supplementary Figure 2. Pathway enrichment analysis of the whole transcriptomic response induced by either *Mav* or *Mtb*.
(A-B) The top 20 most significantly enriched IPA pathways based on the whole host transcriptomic response consisting of all genes down- or upregulated in macrophages infected with *Mav* (A) or *Mtb* (B) compared with uninfected controls. The enriched pathways were ranked by -log 10 p-value of gene enrichment.

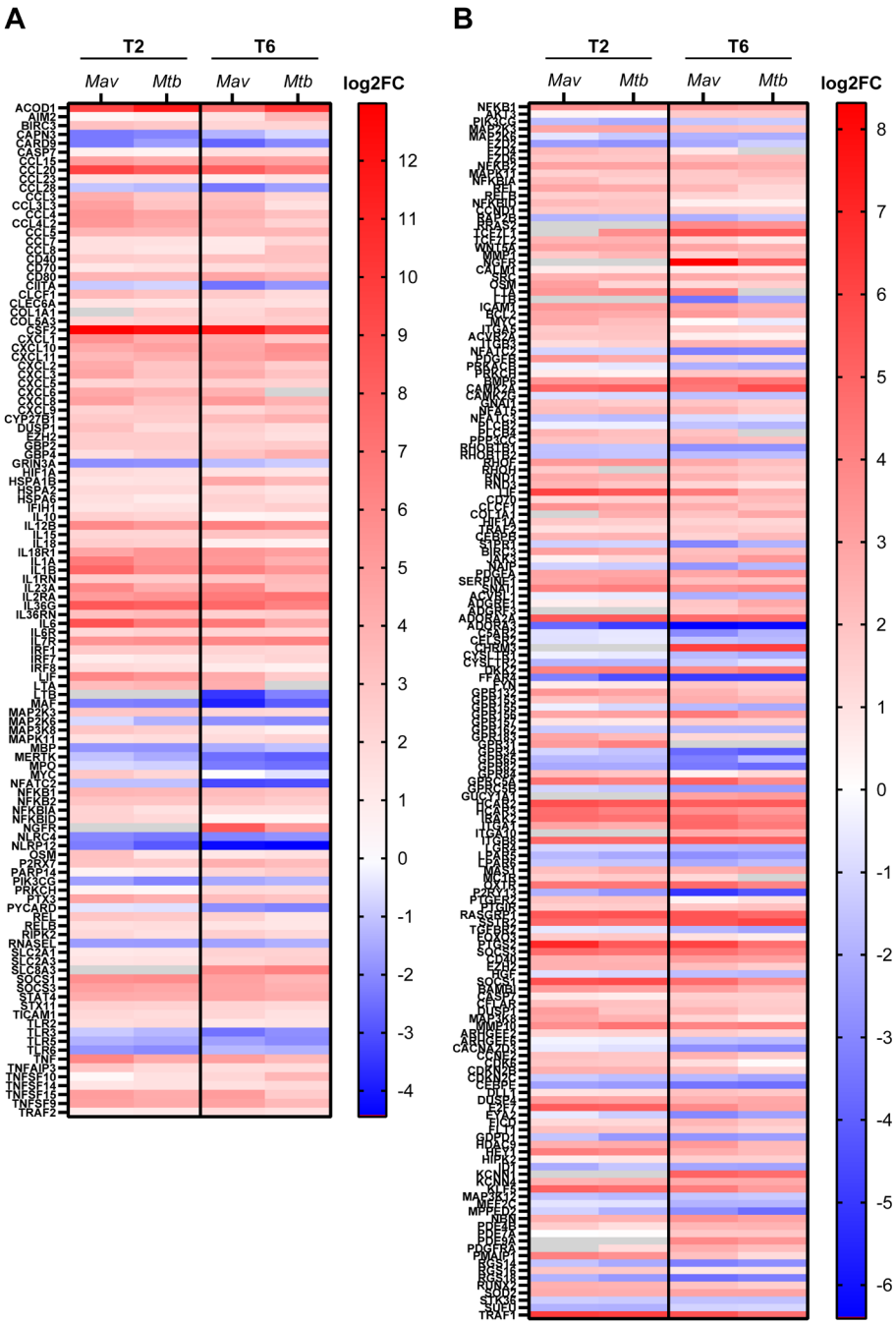

Supplementary Figure 3. Expression patterns of DEGs belonging to the cytokine response or disease-related response commonly induced by *Mav* or *Mtb*.
(A-B) Heatmap showing the expression patterns of 114 DEGs belonging to the cytokine response (A) or 164 DEGs associated with disease pathways (B) commonly induced by *Mav* and *Mtb* in

comparison to uninfected controls. Grey box indicates no expression values could be determined.

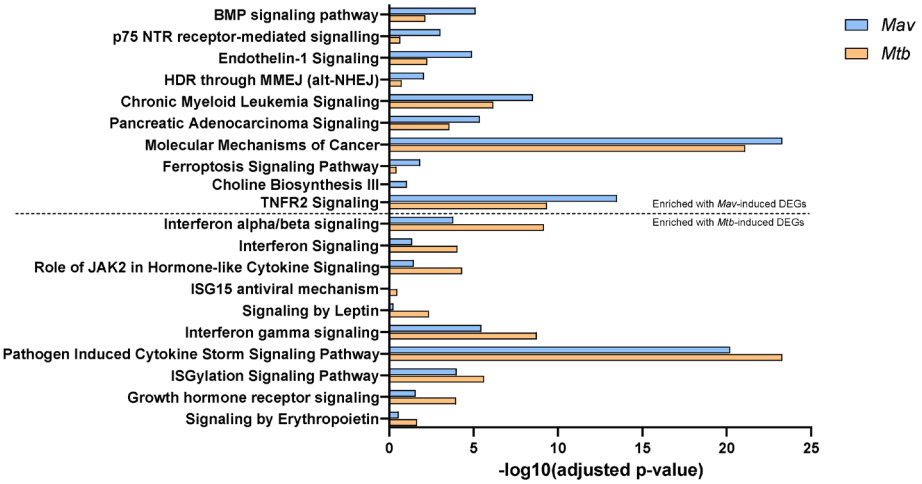

Supplementary Figure 4. Pathway analysis reveals only subtle differences in host signaling between *Mav*- and *Mtb*-infected macrophages.
The top 10 most significantly enriched IPA pathways based on the genes significantly affected in macrophages infected with either *Mav* (above dotted line) or *Mtb* (below dotted line) compared with uninfected controls, also showing the -log 10 p-value of gene enrichment values for the other infection. The enriched pathways were ranked by -log 10 p-value of gene enrichment.

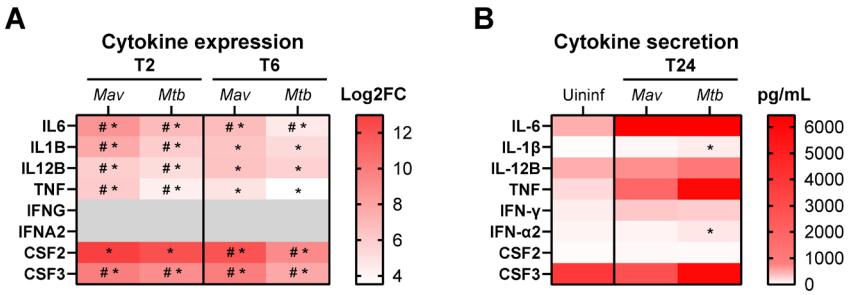

Supplementary Figure 5. Validation of cytokine expression by assessment of cytokine secretion by macrophages infected with *Mav* or *Mtb*.
(A) Heatmap showing the expression patterns of *IL6*, *IL1B*, *IL12B*, *TNF*, *IFNG*, *IFNA2*, *CSF2* and *CSF3* that were differentially regulated in Mav-infected macrophages at 2 (T2) and/or 6 (T6) hours post-infection, compared to uninfected or *Mtb*-infected macrophages. **(B)** Heatmap showing secretion of IL-6, IL-1β, IL-12B, TNF, IFN-γ, IFN-α2, CSF2 and CSF3 measured in supernatants of *Mav*- and *Mtb* infected macrophages collected 24 hours post-infection by the Luminex assay. Shown is the median from three donors.
Asterisk (*) indicates differential expression/secretion when compared to uninfected controls, whereas number sign (#) indicates differential expression/secretion between *Mav* and *Mtb*.